Title: Antagonistic impacts of benthic bioturbator species: interconnected effects on sedimentary properties, biogeochemical variables, and microbial dynamics

Authors: J. Morelle[1,7*], A. Huguet[3], A. Richard[4], A.M. Laverman[2], C. Roose-Amsaleg[2], E. Parlanti[4], M. Sourzac[4], V. Mesnage[5], N. Lecoq[5], J. Deloffre[5], E. Viollier[6], O. Maire[4] and F. Orvain[1]

Affiliations:

[1] Univ. Caen, FRE 2030 BOREA, CNRS-7208, IRD-207, MNHN, Sorbonne Université, UCBN, UA. Caen, France

[2] Univ. Rennes, CNRS, ECOBIO [(Ecosystèmes, biodiversité, évolution)] - UMR 6553, Rennes, France

[3] Sorbonne Université, CNRS, EPHE, PSL, UMR 7619 METIS, Paris, France

[4] Univ. Bordeaux, CNRS, EPOC, EPHE, UMR 5805, F-33600 Pessac, France

[5] Normandie Univ, UNIROUEN, UNICAEN, CNRS, M2C, 76000 Rouen, France

[6] IPGP, Paris, France

[7] Present address: Department of Biology and CESAM – Centre for Environmental and Marine Studies, University of Aveiro, Campus de Santiago, Aveiro, 3810-193, Portugal

* Corresponding author: jerome.morelle@ua.pt ; ORCID: 0000-0003-2167-818X

Abstract:

Macrofaunal species inhabiting intertidal mudflats and performing intense bioturbation are considered as ecosystem engineers, since they profoundly influence their physical, chemical, and biological environments. Nowadays, to complete our knowledge on the effect of bioturbation processes on the surrounding environment, interdisciplinary approach is essential to unravel their complex intertwined effects on intertidal mudflats. In this study, the effects of bioturbators on sediment properties, biogeochemical variables, and microbial dynamics (microphytobenthos, bacteria and archaea) were investigated. To this end, manipulation experiments were carried out in an intertidal mudflat of the Seine Estuary (France) by revamped the abundance of the two dominant bioturbators, *Scrobicularia plana* and *Hediste diversicolor*, in winter and late summer. Results showed that the presence of *H. diversicolor* in winter had a significant effect, with a significant increase in bed level accretion and microbial nitrate reduction rates. In contrast, the presence of *S. plana* showed no significant impact on sediment properties, most likely due to a reduced bioturbating activity at low temperature. In summer, both ecosystem engineers strongly influenced their surrounding environment but with opposite effects. The intense reworking of the sediment surface by *S. plana* limited microbial growth and enhanced erosion processes. Conversely, the presence of *H. diversicolor* favoured sediment accretion and enhanced microbial growth. Overall, this interdisciplinary study confirms the importance of these two ecosystem engineers in temperate estuarine mudflats by highlighting their simultaneous and intertwined effects on the sedimentary, physicochemical, and biological features. This confirms the importance of actively considering ecosystem engineers when restoring the natural habitats of tidal flats to cope with the different vulnerability risks related to global warming (sandification of estuarine sediments, disappearance of productive mudflats, sea level rise, vulnerability to storms and erosion).

Keywords: biogeochemical cycles; ecosystem engineers; microbial communities; microphytobenthos; organic matter; sediment

1. Introduction

Intertidal mudflats comprise a diverse range of sedimentary habitats that serve as nursery and refuge areas for various migratory and resident species, and play a crucial role in the biogeochemical processes of estuaries and coastal ecosystems (Paterson et al. 2019). In these systems, microphytobenthic biofilms (MPB) represent the main primary producer, supporting a complex trophic network where benthic invertebrates are the primary food source for valuable consumers, such as fish and shorebirds (Dauwe et al. 1998; Underwood and Kromkamp 1999). Moreover, MPB plays an essential role in biogeochemical dynamics and sediment stabilization through the secretion of extracellular polymeric substances (EPS) (Stal 2010; Hope et al. 2020).

The growth and productivity of MPB are influenced by various environmental factors (Underwood and Kromkamp 1999). In nutrient rich ecosystems, MPB productivity is mainly driven by the strong variation in light intensity at the sediment surface (Behrenfeld et al. 2004; Cartaxana et al. 2011) and the substantial seasonal variation in temperature impacting both MPB and biochemical reactions (Raven and Geider 1988; Davison 1991; Claquin et al. 2008). Nevertheless, nutrient concentrations at the water-sediment interface, influenced by water fluxes and organic matter (OM) mineralization through microbial respiration, continue to exert a discernible influence on MPB (Aller and Cochran 2019), along with salinity, pH, oxygen levels, currents, and sediment properties (Underwood and Kromkamp 1999; Juneau et al. 2015; Redzuan and Underwood 2021). Finally, biological disturbances of the sediment-water interface (i.e. especially through macrofaunal bioturbation) may lead to drastic changing in sediment abiotic conditions, and thus indirectly influence MPB biomass and productivity, with far-reaching consequences for the intricate trophic network through bottom-up ecological cascades.

Bioturbation by macrofaunal species includes sediment reworking (mixing sediment particles) and bioirrigation (transport of solutes) processes, which are mainly related to behaviours burrowing, locomotion, and feeding activities (Kristensen et al. 2012). The impacts of macrofaunal activities on the MPB and its surrounding environment are linked to both direct (trophic) and indirect interactions (Jones et al. 1994; Bruno and Bertness 2001; Crain and Bertness 2006; Ubertini et al. 2012; Van De Koppel et al. 2015). Despite the negative effects of macrofaunal bioturbation related to grazing and sediment surface disruption, bioturbating macrofauna has also been shown to positively influence microbial processes (Swanberg 1991; Orvain et al. 2004; Chennu et al. 2015, 2017; Eriksson et al. 2017; D'Hondt et al. 2018). Therefore, by facilitating oxygen and solute exchange at the sediment-water interface, bioturbation activities enhance the influx of dissolved OM (DOM), aerobic OM remineralization, and nutrient cycling. Bioturbation also promotes bacterial growth by accelerating solute and particulate exchanges at the water-sediment interface, (Aller 1988; Boudreau and Jorgensen 2001; He et al. 2019). Oxygenation and sediment surface irrigation by bioturbation may also modify the redox boundary, thus influencing the quantity and quality of sedimentary OM (Fanjul et al. 2015). This, in turn, can be influenced by the structure, metabolic rate, and functioning of benthic communities (Dauwe et al. 1998; Oleszczuk et al. 2019). The chemical composition and dynamics of sedimentary and dissolved OM are thus impacted, especially because the properties of pore-water DOM produced during biodegradation processes have been shown to be mainly dependent on sedimentary OM sources (Burdige and Komada 2015; Derrien et al. 2019). Overall, the influence of bioturbation on the surrounding environment is significant, regulating sediment dynamics, bed erodibility, and biogeochemical processes, with both positive and negative effects on the microbial compartment. Some macrofauna species with high bioirrigation activity can be particularly influential, especially in cohesive sediments, where solute diffusion is limited. These positive and negative effects are expected to exhibit temporal variability as macrofaunal

bioturbation has been shown to be modulated by temperature, with more pronounced effects in spring, summer, and early autumn (Admiraal and Peletier 1980; Colijn and Dijkema 1981; Underwood 1994; Stal and de Brouwer 2003; Orvain et al. 2014; Cozzoli et al. 2018).

The impacts of benthic macrofaunal bioturbation and its regulatory effects on various properties of the surrounding environment (e.g., sediment composition, OM, nutrient recycling, recruitment of macrofaunal spats, bacterial and MPB growth, or consumption rates) have been extensively studied. However, complex interactions among all physicochemical and biological components give rise to intricate "bottom-up" and "top-down" forces that are not yet fully understood. Understanding these interactions is essential for maintaining the balance and value of the ecosystem services they provide in intertidal mudflats. Bioturbation by benthic macrofauna and its effects, which are vital drivers of mudflat structure and function, are critical elements to be considered in ecological studies and environmental management strategies. Given the findings of previous studies, it is crucial to investigate the synergistic effects. To achieve this goal, interdisciplinary studies offer a holistic and comprehensive approach that provides insights into the complex and interconnected relationships within trophic networks.

In this context, the present study aimed to investigate the effects of two dominant benthic macrofaunal species in intertidal mudflats on different components of the surrounding environment, including bed topography, sediment composition, biogeochemical processes, and microbial and MPB activities. The selected representative site is a temperate intertidal mudflat located downstream the Seine Estuary (northwest France). The selected ecosystem engineers (fig. 1) were the bivalve *Scrobicularia plana*, which is predominantly responsible for surface sediment reworking (Zwarts et al. 1994; Orvain 2005), and the annelid *Hediste diversicolor*, which is primarily involved in gallery bioirrigation (François et al. 2002; Passarelli et al. 2012; Richard et al. 2023). *S. plana* is a widely distributed filter feeder characterized by long siphons that enable it to bury itself in sand or mud. This species thrives at high densities along coastlines and estuaries in northern Europe, the Mediterranean, and West Africa (Santos et al. 2011). *H. diversicolor* is a versatile predator that forms distinctive U-shaped burrows in sand and mud, featuring a mucus net at the entrance. This species creates a water current within its tube to draw particles through the net. Native to the northeast Atlantic, *H. diversicolor* range extends from the Baltic Sea to the Mediterranean and has been introduced to the northwest Atlantic (Einfeldt et al. 2014).

Although field observations are typically conducted to study various components of a trophic network simultaneously (Weerman et al. 2011), autocorrelation and confounding factors can complicate the mechanistic understanding of intertwined processes. Therefore, field studies with addition of macrofauna and manipulative experiments are relevant to assess the role of one ecological factor, among others, in bio-mediated sediments (Montserrat et al. 2009; Van Colen et al. 2010; Donadi et al. 2013). As such, a manipulative field experiment was established with enclosures buried in sediments, each containing different densities of macrofauna. Subsequently, a wide range of sedimentary, microbial, and biogeochemical parameters were concurrently measured. This study was conducted during two contrasting periods in terms of biotic and abiotic conditions: late winter (February) and late summer (September). The main hypothesis posited that the two target organisms (*H. diversicolor* and *S. plana*), which typically coexist in intertidal mudflats, would have antagonistic effects on bed erodibility (stabilizer vs. destabilizer) and sediment mixing in superficial layers (dissolved exchanges vs. particulate exchanges). The positive influence of the presence of *H. diversicolor* on MPB growth was anticipated because of its impact on sediment stability and bioirrigation activities within its galleries (Morelle et al. 2021; Richard et al. 2023). Conversely, it was expected that the presence of *S. plana* would limit MPB growth owing to disruption of the

sediment surface (Richard et al. 2023). Furthermore, the OM quality and quantity are expected to be modified in the presence of ecosystem engineers, particularly in the dissolved phase (DOM), owing to enhanced oxygenation and sediment surface irrigation through bioturbation, especially in the presence of the gallery bioirrigator *H. diversicolor*.

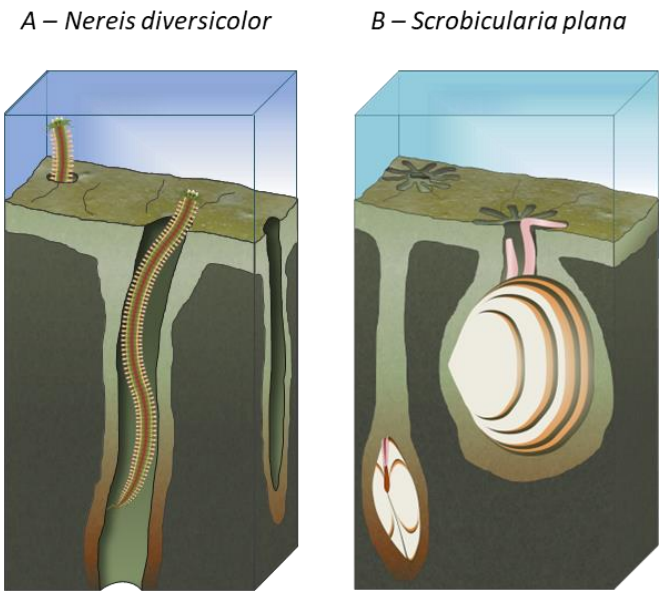

Figure 1. Representation of the two species studied in this work. The annelid *Hediste diversicolor* (A) is primarily involved in gallery bioirrigation while the bivalve *Scrobicularia plana* (B) is predominantly responsible for surface sediment reworking. Copyright: illustrations from Bastien Chouquet for the MELTING POT(ES) project.

2. Material and Methods

2.1. Sampling site and experimental design

Field experiments were conducted in the European temperate macrotidal estuary of the Seine River at an intertidal site (fig. 2). Bivalves (shell length between 40 and 43 mm) and polychaetes (body length of approximately 90 mm) were collected by hand at the same location. Specimens were stored in two distinct tanks, each approximately 100L in capacity, filled with natural seawater and sediment from the sampling site (~10 cm in depth). The water was oxygenated using air pumps, tide conditions were absent, and no supplementary food was provided. The tanks were conserved for one week in a temperature-controlled room at 12°C for winter experiment and at 21°C for late summer experiment with exposure to natural ambient light.

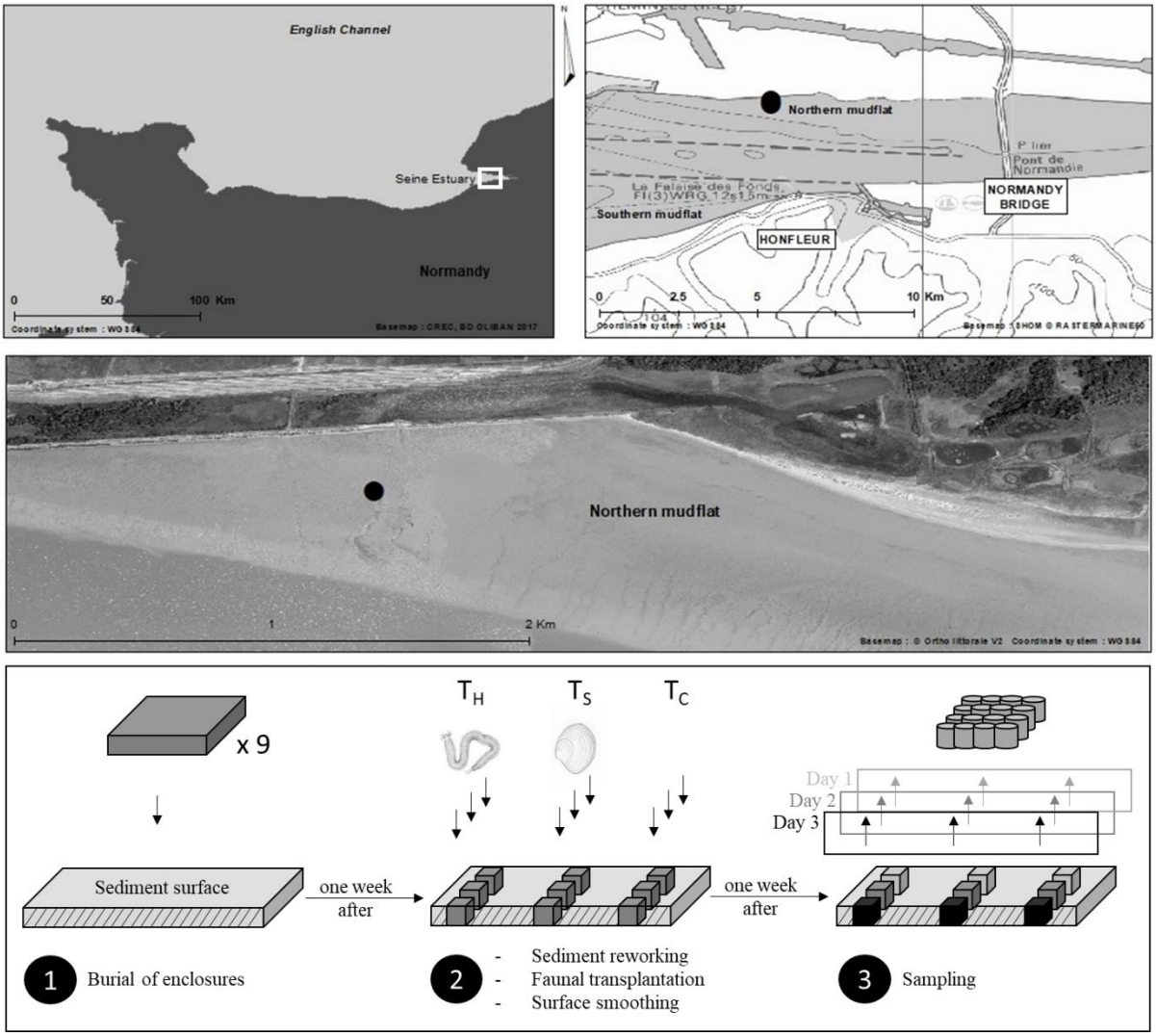

Figure 2. Location of the Seine Estuary (Normandy, English Channel, France) with the sampling site located in the northern mudflat (49° 27' 01.6'' N; 0° 12' 20.0''E). The experimental design consisted in the burial of nine enclosures. One week later, sediment inside enclosures were reworked by hand and transplanted with macrofauna (*Hediste diversicolor*: T_H; *Scrobicularia plana*: $T_{S;}$ and nothing for control: Tc). After burial of fauna, sediment surfaces were smoothed and one week later, several cores were sampled over 3 days from each enclosure (1 replicate for each treatment per day: T_H, T_S or T_C).

At the beginning of the experimentation, nine experimental plots (stainless steel enclosures; 50 × 50 × 20 cm) were buried at the study site so that the top of the enclosures was precisely at the same level than the sediment surface. To avoid additional topographical variation between replicates, enclosures were placed at a distance of 1 m from each other in a homogeneous area of the mudflat (fig. 2). Sediment in each plot was then gently reworked by hand up to a depth of 20 cm and the faunal enrichment was then achieved by direct addition of the organisms in subsurface (2-3 cm) within the sediment bed. Each specimen was individually added to ensure vitality and to accurately record the number of individuals in each replicate. In February, the enrichment represented an addition of 35 individuals per replicate (140 ind m^{-2}) while in September, the enrichment represented an addition of 110 individuals (440 ind m^{-2}). The final densities represented the maximum densities observed at the study site during the sampling periods (comm. pers. Chloé Dancie – "Cellule de Suivi du Littoral

Normand | CSLN"). In order to have a net monospecific dominance for the two treatments with faunal addition, three replicates were enriched with *S. plana* (treatment T_S) and three others were enriched with *H. diversicolor* (treatment T_H). After animal addition, the sediment surface was flattened in all experimental units, to assess later the effects of bioturbation on bed level. Sediments in control plots were reworked by hand and flattened similarly but without faunal addition (control treatment T_C). The process of the aforementioned steps was completed within one low-tide period. After one week under *in situ* conditions, the samplings were conducted during neap tides, when low-tide coincided with mid-day conditions. The different enclosures were sampled over 3 days due to tidal and safety conditions in intertidal zones. Each day, measurements were performed in successive samplings for one line of enclosure units (fig. 2), including one replicate of each treatment (T_C, T_H, T_S) by following the same sampling method. In addition, the natural state of the mudflat sediment was also sampled each day and assigned as natural treatment (T_N). The experiments were performed in the two most contrasted periods of the year in late winter (February 9th - 26th, 2018) and late summer (September 18th - October 4th, 2018). For that, enclosures were removed after the winter experiment and the whole process was repeated for the summer experiment.

2.2. Sampling methods

The sampling protocol followed was schematically described in figure 3. Due to the interdisciplinary approach and the number of measurements requiring a relatively high quantity of sediment within each enclosure, the sampling strategy followed a precise protocol which was not random but statistically relevant (see 2.4). Throughout each manipulative experiment, environmental parameters (light intensity, temperature profile, water elevation) were recorded *in situ* at the study site, outside the enclosures. Light intensities were recorded every 15 min using an Onset Hobo UA-002 Pendant light/temperature data logger placed 15 cm above sediment surface. Vertical temperature profiles were performed every 15 min using five submersible temperature data loggers (Onset Hobo® Pendant® UA-001) placed at 0, 2, 5, 10 and 15 cm depth using a holder buried in the sediment. Water elevation was measured using a NKE© Altus based on a piezo-resistive pressure sensor (accuracy was +/-60 mm while resolution was +/- 8 mm). This instrument was set up to achieve one measurement every 30 seconds.

For each treatment with enclosure (T_C, T_H, T_S), the bed level variation was estimated to evaluate the bed accretion or erosion. To this aim, a measurement of the height distance between the enclosure borders (initial sediment surface after flattening) and the sediment surface was performed by using a calliper on 16 fixed points evenly distributed over the surface with a step of 10 cm from each other (fig. 3; total surface of 0.25 m²).

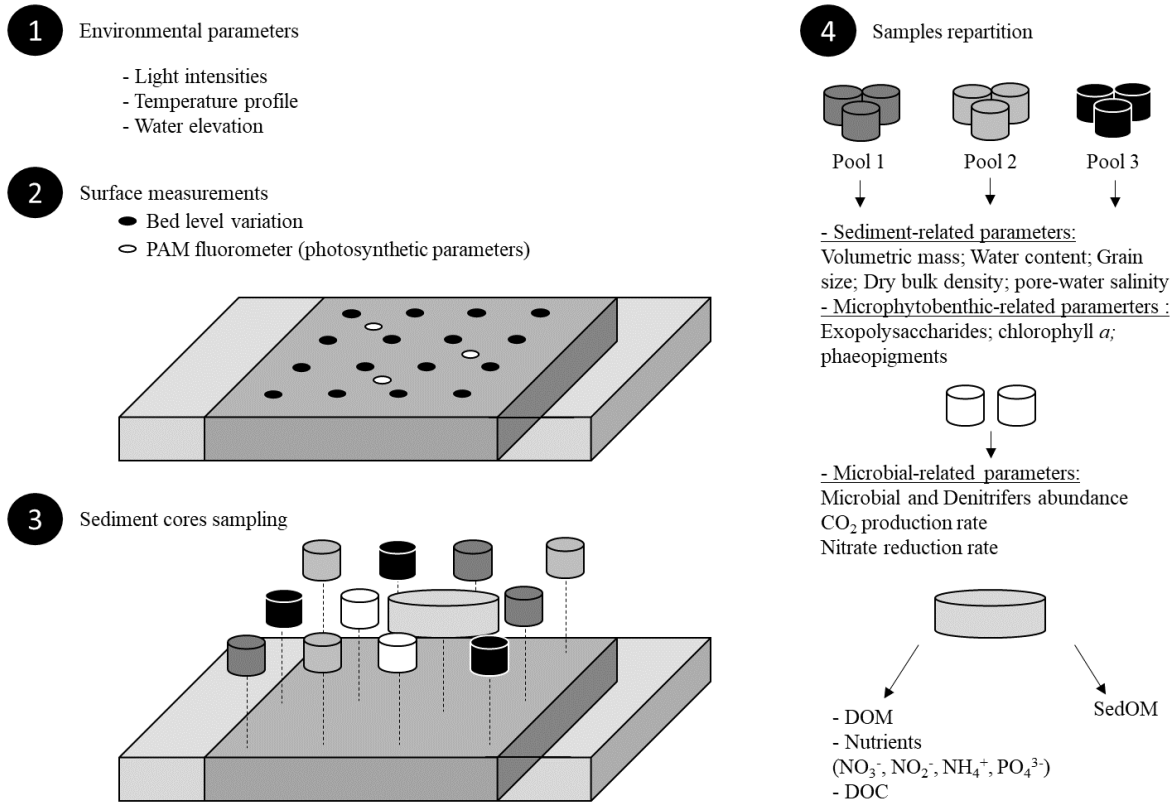

Figure 3. Schematic representation of the successive actions carried out during each sampling day. The environmental parameters (light intensities, temperature profiles and water elevation) were measured continuously. The first measurements made were the variation of the bed level which was measured at 16 different points and the PAM fluorometer made at 3 different positions. These two measurements did not disturb the sediments. Then, the sediment cores were sampled, and the sediment was distributed and conditioned for future analysis of the parameters considered in this study.

Immediately after bed level variation measurement, chlorophyll fluorescence was measured in triplicate (*n*=3) at the sediment surface within each enclosure. This was performed using a Fiber-PAM fluorometer (PAM-control unit and WATER-EDF-universal emitter detector unit; Walz, Effeltrich, Germany) following the method fully described in Morelle et al. (2020). Each replicate was exposed to nine actinic irradiance steps from 0 to 168 µmol photons m^{-2} s^{-1} in winter and from 0 to 1130 µmol photons m^{-2} s^{-1} in summer. These irradiance ranges were chosen as they match with those of the light environment of each season (Morelle et al. 2018). The treatment of the fluorescence data using the model of Eilers and Peeters (1988) allowed assessment of photosynthetic parameters, i.e., the maximum effective quantum yield of the PSII (F_V/F_M), the photosynthetic efficiency (α; relative unit), the optimal irradiance for photosynthesis (E_{opt}; µmol photons. m^{-2}. s^{-1}), the relative maximum electron transport rate ($rETR_{max}$; relative unit), and the saturation coefficient of light (E_k; µmol photons. m^{-2}. s^{-1}).

Afterwards, the sediment was sampled through core extraction. Two plexiglass rings (4 cm in diameter down to a depth of 1 cm) were sampled to study the microbial activity and abundance. A fraction of 3 ml from the first ring was stored at -80°C for bacterial abundance determination. The remaining sediment from the first ring and the second ring were kept at 4 °C for the microbial activity experiments. Then, nine cores (2.4 cm in diameter

down to a depth of 1 cm) were collected and distributed into 3 pools, each representing 13.5 ml of sediment which were cautiously homogenised. For each pool, a fresh sediment aliquot (5 ml) was used for sedimentary analyses. Another sediment aliquot (5 ml) was used to determine exopolysaccharides concentrations. The last sediment aliquot (1.5 ml) was stored at -20 °C for analyses of photopigment concentrations. A last sediment core (9.3 cm in diameter down to a depth of 30 cm) was sampled to analyse the pore-water vertical profiles. Interstitial pore-water samples were extracted using Rhizon samplers (pore size 0.15 µm mean) and polypropylene syringes at a depth interval of 0 – 1 cm (for more information see Seeberg-Elverfeldt et al. (2005)). Each pore water sample was divided into two aliquots and stored in the dark at 4°C. The first aliquot of pore-water was kept for measuring nutrient ($Si(OH)_4$, PO_4^{3-}, NH_4^+, NO_2^-, and NO_3^-) and dissolved organic carbon (DOC) concentrations. The second aliquot was stored for DOM spectroscopic analyses. The 0 – 1 cm depth interval of the core was then sliced and frozen at -20 °C, freeze-dried, ground, and homogenised before sedimentary organic matter (SedOM) characterization.

2.3. Analytical methods

2.3.1. Sediment-related parameters.

To estimate the sediment-related parameters, each aliquot of sediment sampled from the pooled cores (5 ml) was weighted to estimate the volumetric mass and was kept at -20°C. After freeze-drying for 24h, the water content (ω; %) was determined as a percentage of water relative to the total fresh weight. Subsequently, sediment was used for granulometric analysis. For that, sediments were digested in 6% hydrogen peroxide for 48 h to remove OM. The grain size distribution was then measured on subsamples using a LS Coulter particle size analyser. The mud sediment fraction was estimated as the percentage of silt particles < 63 µm (% of fine particles) and the median grain size diameter was estimated from cumulative percentage histogram. The dry bulk density (C_{sed}, kg m^{-3}) was then estimated from ω_D (Water weight / Dry weight × 100) and grain density (γ_s; kg m^{-3}) according to the equation $C_{sed} = (\gamma_s \text{ x } 1000)/[(\omega_D/100) \text{ x } \gamma_s + 1000]$.

Nutrients (NO_3^-, NO_2^-, NH_4^+, PO_4^{3-}) and DOC concentrations were obtained from the pore-water samples. Dissolved/reactive silica ($Si(OH)_4$) concentrations were determined from filtered samples by spectrophotometry (Koroleff, (1983), silico-molybdenum blue method) using a QuAAtro (Seal Analytical) continuous segmented flow analyzer. Dissolved nitrates ($N\text{-}NO_3^-$) and nitrites ($N\text{-}NO_2$) concentrations were analysed using a Gallery™ Discrete Analyzer (ThermoFisher scientific, Waltham, Massachusetts, USA). The reactive phosphate $P\text{-}PO_4^{3-}$ and the dissolved ammonium $N\text{-}NH_4^+$ were analysed using a Technicon Auto-analyzer II, with a detection limit of 14 µg L^{-1} and 42 µg L^{-1}, respectively for $P\text{-}PO_4^{3-}$ and $N\text{-}NH_4^+$ and a standard error lower than 5%. DOC was analysed using a "TOC Shimadzu 5050" carbon analyser with two injections or three if the standard error was higher than 5%.

2.3.2. Microphytobenthos-related parameters.

Colloidal and bound fraction of exopolysaccharides were immediately separated from the sediment aliquot (5 ml) using Dowex and conserved at -20°C for analyses following the method fully described in Morelle et al. (2020). The concentrations of high molecular weight (HMW) exopolysaccharides (after separation from Low-MW EPS in 70% Ethanol) were then measured for the colloidal (C-EPS) and bound (B-EPS) fractions. Carbohydrate contents were estimated using sulfuric acid and phenol with glucose as a standard (Dubois et al.

1956). Protein contents were estimated using the Bradford assay with bovine serum albumin (BSA) from Sigma-Aldrich as standard (Bradford 1976).

After freeze drying, photopigments were extracted from 1g of dry weight (DW) sediment in 90% acetone and the fluorescence of the supernatant was measured using a Turner Trilogy fluorometer (Turner Designs, Sunnyvale, California, USA). Chlorophyll *a* (chl *a*) and phaeopigments concentrations were calculated from the fluorescence values obtained before and after acidification following the method of Lorenzen (1967). The phaeopigment contents were expressed as a percentage of total photopigments.

2.3.3. Microbial-related parameters.

Microbial abundances were obtained after DNA extraction from approximately 0.5 g of fresh surface sediment (0-1 cm) according to the protocol detailed in Hellequin et al. (2018) modified from Quaiser et al. (2014). They were determined by quantitative PCR targeting generalist (*16S rRNA* genes of bacteria or archaea) and functional genes as Clade I *nosZ* gene and Clade II *nosZ* gene for N_2O-reducers and calibrated with standard positive DNA. For the *16S rRNA* gene, the standard for Bacteria was DNA of *Pseudomonas fluorescens* SBW25 using primers 63f and BU16S4 (Muyzer et al. 1993; Marchesi et al. 1998) and PCR fragment cloned of *Nitrosophaera viennensis* for Archaea with primers Arch806F and Arch915R (Takai and Horikoshi 2000). As in Jones et al. (2013), the standards for *nosZ* genes corresponded to PCR fragment cloned of *Bradyrhizobium japonicum* USDA 110 for Clade I and *Gemmatimonas aurantiaca* T-27 for Clade II. No-template controls were performed in duplicate and assays in triplicate. Amplifications were performed in a Lightcycler 480 (LC480, Roche) using Sensyfast Sybr no rox kit (Biotechnofix). Analyses were carried out with LC480 software (release 1.5.1) consisting in melting curves and absolute quantification by second derivative maximum analysis method allowing the determination of the crossing points (Cp). We defined the detection limit as fluorescent signals with at least 5 Cp below the signal of the no-template controls.

The potential of sedimentary organic carbon degradability was determined in batch incubations by measuring the CO_2 production rate under anoxic conditions. To this end 5 ml of the sediment was placed in a serum bottle with 20 ml of water collected on site (filtered at 0.2 µm). The headspace was replaced by Argon to create anoxic conditions and 500 µM nitrate ($NaNO_3$) was added. Batches were incubated at 20 °C and agitated (150 g). Samples from the headspace were analysed for CO_2 using a micro-GC Agilent 3000 (SRA Instrument) at the beginning of the incubation, after 2 hours and 4 hours. The CO_2 production was determined over the 4 hours and expressed as CO_2 production in $gDW^{-1}\ h^{-1}$.

The potential nitrate reduction rates were estimated from the sediment samples by performing a flow-through reactor experiment. For description of the method see (Laverman et al. 2006, 2012). The reactors were supplied with anoxic saline water (adapted to the onsite salinity) containing 5 mM of $NaNO_3$ at a flow rate of 3 ml h^{-1} with a peristaltic pump and incubated at a constant temperature (20°C). The reactors were run for approximately 30 hours, allowing determination of nitrate consumption using the *in situ* available carbon present in the sediment. NO_3^-, NO_2^-, NH_4^+ concentrations were determined via a Gallery (Thermofisher) from outflow samples collected at 2-hour intervals. Samples from the input solution were also collected and analysed for the exact nitrate concentrations. Potential nitrate reduction rates were then calculated and expressed in nmol NO_3^- per cm^3 of fresh sediment per hour.

292 **2.3.4. Organic matter-related parameters.**

293 DOM spectroscopic analyses were performed on filtered samples. Excitation-emission matrix (EEM)
294 fluorescence spectra were acquired, depending on the pore water volume available, in 1 or 0.5 cm path length
295 quartz SUPRASIL® QS cuvettes (Hellma) regulated at 20 °C, using a Jobin-Yvon Fluorolog FL3-22
296 spectrofluorometer in ratio mode with 4 nm bandwidth for both excitation (250-410 nm, 10 nm intervals) and
297 emission (260-700 nm, 1 nm increments and 0.5 s integration time) (Parlanti et al. 2000). Samples were diluted, if
298 necessary, to avoid inner filter effects, and their spectra, obtained by subtracting an ultrapure water (Milli-Q,
299 Millipore) blank spectrum, were instrumentally corrected as described previously (Huguet et al. 2009). The
300 subsequent fluorescence indices were computed to provide insights into the origin, maturity, and transformation
301 of dissolved organic matter (DOM). The humification index (HIX), indicative of the aromaticity level and maturity
302 of DOM (Zsolnay et al. 1999), was determined based on the position of the emission spectra. Specifically, the
303 upper quarter area (435 - 480 nm) of the usable emission peak was divided by the lower usable quarter area
304 (300 - 445 nm). This calculation facilitated the differentiation between strongly humified organic material,
305 primarily of terrestrial origin (10 < HIX < 16), and autochthonous organic material (HIX < 5). Another key
306 fluorescence index, the fluorescence index (FI), expressed as f_{450}/f_{500}, represents the ratio of fluorescence intensity
307 at the emission wavelength 450 nm to that at 500 nm with an excitation wavelength of 370 nm. This index aids in
308 discriminating between microbial (FI = 1.9) and terrestrial sources (FI = 1.3) of aquatic DOM (McKnight et al.
309 2001). Additionally, the biological index (BIX), serving as a proxy for fresh autochthonous DOM production
310 associated with biological activity (Huguet et al. 2009), was computed at an excitation wavelength of 310 nm. It
311 involves dividing the fluorescence intensity emitted at an emission wavelength of 380 nm by that emitted at 430
312 nm. BIX values exceeding 0.8 indicate a predominantly autochthonous origin of DOM and the presence of freshly
313 released organic matter into the water, while lower BIX values (0.6 – 0.7) suggest moderated DOM production in
314 natural waters.

315 The elemental (organic carbon, nitrogen) and isotopic ($\delta^{13}C$) analyses of the SedOM were performed on
316 sediment samples after being decarbonated as previously described (Thibault et al. 2019).

317 Lipid extractions were performed using on average 20 g of sediment. Samples were ultrasonically
318 extracted at room temperature with a dichloromethane (DCM)/ methanol (MeOH) mixture (5:1) for 10 minutes (3
319 times). Each extraction was followed by centrifugation (3500 rpm, 10 minutes) and pooling of all extracts. The
320 total lipid extract was rotary evaporated and separated into three fractions of increasing polarity on a column of
321 activated silica: (i) 30 ml of heptane; (ii) 30 ml of heptane:DCM (1: 4, v:v); (iii) 30 ml of DCM:MeOH (1:1, v:v).
322 Each fraction was then rotary evaporated.

323 The *n*-alkanes, contained in the first fraction, were analysed by gas chromatography coupled to a mass
324 spectrometer (GC–MS) using an Agilent Network 6890 GC System coupled with a 5973 Mass Selective Detector,
325 as previously described by Coffinet et al. (2017). 1.1 µg of internal standard (n-tetracosane-d_{50}; Sigma-Aldrich)
326 was added just before injection. The different *n*-alkanes were semi-quantified based on their retention time, after
327 extraction of the characteristic *m/z* 57 fragment.

328 The *n*-alcohols were analysed in the third fraction containing the polar compounds. Before GC-MS
329 analysis, the fraction was dissolved in DCM and derivatized by adding 10% in volume a solution of
330 N,O- bis(trimethylsilyl)trifluoroacetamide – Trimethylchlorosilane 99:1 (Grace Davison Discovery Science,
331 USA). The separation was achieved with the same equipment as above. The GC oven initial temperature was set

to 70 °C (maintained for 1 min), increased to 130 °C at 20°C min^{-1} and then to 320 °C at 4 °C min^{-1} (maintained for 25 min). Samples were injected in split mode (ratio 30:1), the injector being at 280 °C. 1.5 µg of internal standard (5α-cholestane; Sigma-Aldrich) was added just before injection. The silylated *n*-alcohols were semi-quantified based on their retention time, after extraction of the characteristic *m/z* 75 fragment.

The relative abundances of *n*-alkanes and *n*-alcohols were used to discriminate OM sources in natural environments. Thus, terrestrial vascular plants are dominated by odd long-chain *n*-alkanes (C_{23}-C_{35}), with C_{27}, C_{29} and C_{31} being the dominant homologues (Bianchi and Canuel (2011) and references therein), and by long-chain *n*-alcohol (≥ C_{20}) (Eglinton and Hamilton 1967). In contrast, algae and bacteria are dominated by short-chain *n*-alkanes, with C_{15}, C_{17}, or C_{19} predominance, and short-chain *n*-alcohols (C_{12}-C_{18}). Submerged macrophytes have an intermediate composition, with a predominance of mid-chain *n*-alkanes (C_{21}, C_{23} or C_{25} ; Bianchi and Canuel (2011)). In the following, the relative abundance of C_{27} + C_{29} +C_{31} *n*-alkanes *vs.* odd *n*-alkanes in the range C_{15}-C_{31} will be considered as a proxy of terrestrial OM. Similarly, the relative abundance of long-chain *n*-alcohol (≥ C_{20}) *vs.* total *n*-alcohols (i.e., short (C_{12}-$_{18}$) + long-chain homologues) will be used to estimate the proportion of terrestrial *vs*. aquatic (algal/bacterial) OM (e.g., Vonk et al. (2008)).

2.4. Statistical analyses

In terms of statistical analyses, it was impossible to include the "season factor" since the fauna treatment was not the same at the two seasons. The densities were chosen to be representative of the observed maximum at each specific season in historical surveys of macrozoobenthic communities. The experiments achieved in winter end and summer end must be therefore considered as 2 independent experiments in contrasted conditions to better unravel the effect of the bioturbators on other properties.

For each season, all samples were taken one week after faunal treatments, in a whole 10 × 10 m square experimental study area (one per season) delimited by two perpendicular lines spaced 2 meters apart. The sampling period lasted 3 days. Each day, one replicated square of the 4 treatments was randomly chosen according to the sampling design described in a previous field study (Orvain et al. 2012, 2014), so that day effect cannot bias the analysis. In these squares, surficial sediment was systematically sampled in 1 hour at mid-tide condition to avoid any difference related to the inundation time. No difference was detected between sampling days for all variables.

Concerning spatial independence, a preliminary analysis of spatial autocorrelation was performed to evaluate the independence requirements on the site regarding the two main variables (i.e., sediment composition and chlorophyll content). This allowed to guarantee that the condition of spatial independence was not compromised in the analysis since, at 2 meters of distance between each subunit plot, the hypotheses of null autocorrelation was not rejected. A Durbin-Watson test allowed us to confirm the absence of spatial autocorrelation between sub-units, when applying a regression test between sediment composition and chl *a* content.

After that Shapiro-Wilk normality tests and Bartlett equal variance tests were applied on each parameter of the dataset, statistical analyses were performed by using a one-way ANOVA to compare the 4 treatments (T_C, T_H, T_S, and T_N) using the R software (version 4.0.2). In the case of significant differences in the ANOVA ($p < .05$), Tukey comparison tests were performed with the considered factor to discriminate differences. The non-parametric test of Kruskal-Wallis followed by pairwise-t-tests was used when conditions were invalid. Correlations between parameters were tested using Pearson correlation tests.

3. Results

3.1. Meteorological conditions during sampling and impact of experimental design

Irradiance level varied following the daily cycle with a maximum of 3000 µmol photons m^{-2} s^{-1} for winter and 2600 µmol photons m^{-2} s^{-1} for late summer period except during the 1st day of the survey, where irradiance values reached a maximum of 95 µmol photons m^{-2} s^{-1} (fig. 4). During the low-tide period (lasting ~5.5h), the average values were 1650 µmol photons m^{-2} s^{-1} in winter and 657 µmol photons m^{-2} s^{-1} for late summer period.

A diurnal cycle was also observed for temperature values (fig. 4), which varied between -5.5 and +13.8 °C for winter and between +9.7 and +35.1 °C for late summer period. Maximal values were observed during zenith, while minimal values were observed during the nocturnal low tide. During the winter sampling period, the temperature values in the sediment surface were lower than 0°C, leading to frost events. At 2 cm depth, the range of temperature variation was lower than on the surface with values between -1.3 and +7.2 °C for winter and between +11.3 and +25.1 °C for late summer period (fig. 4).

The impact of the deployment of experimental enclosures was estimated by considering the differences between the control treatment (T_C) and the natural state around enclosures (T_N). A significant difference was observed between T_C and T_N on DOM index and phaeopigments in winter (table 1). For the other parameters and in summer, it was assumed that differences between T_H, T_S, and T_C revealed treatment-related effects and did not result from an experimental artifact.

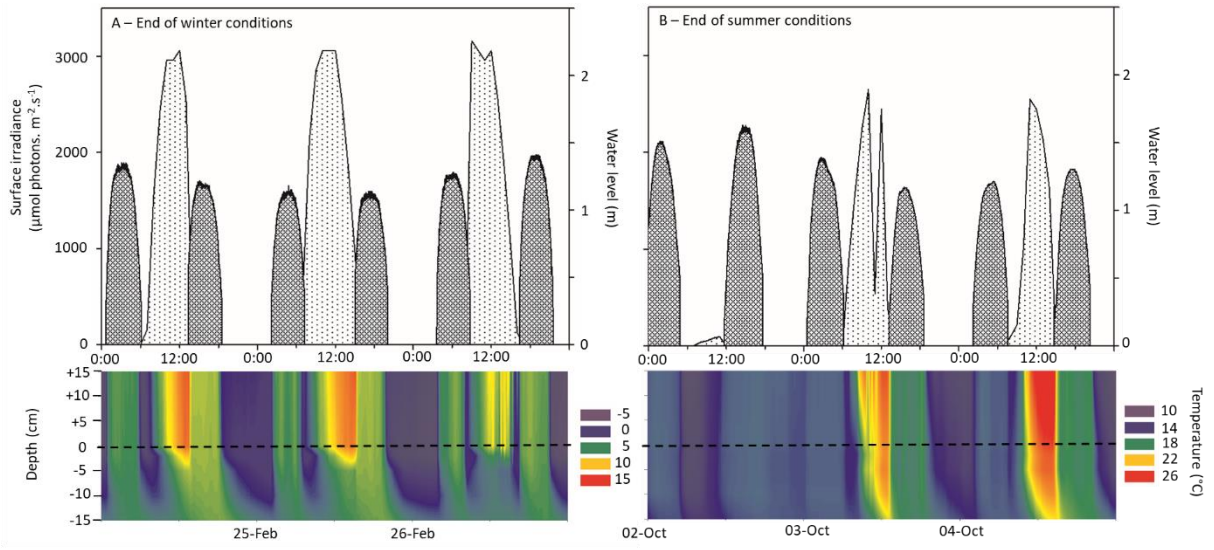

Figure 4. Variation of environmental parameters during the monitoring periods under (A) winter and (B) late summer conditions. With the depth profile of temperature in sediment (°C), surface irradiance (µmol photons m^{-2} s^{-1}) in pale grey, and water level (m) in dark grey.

3.2. Winter conditions

3.2.1. Sedimentary parameters

In each treatment (T_C, T_H, T_S), the bed level variation showed an increase in sediment height (Table 1; Figure 5-A). This sediment accumulation was significantly higher in the presence of *H. diversicolor* with 1.2 ± 0.6 cm compared to the control (0.7 ± 0.7 cm) or in the presence of *S. plana* (0.9 ± 0.8 cm). No other significant

differences were recorded between the treatments for sedimentary parameters, with an average of 14.2 ± 5.3% fine particles (median of 155.7 ± 9.8), a volumetric mass of 1.9 ± 0.1 kg/L, a dry bulk density of 1633.1 ± 47.8 kg/m³, and a water content of 23.6 ± 1.8% (supp. table 1).

The parameters related to the SedOM also showed no differences between treatments (supp. table 1). Total organic carbon (TOC) ranged between 0.07 and 0.37 % while total nitrogen (T_N) was very low between 0.01 and 0.05%. The $\delta^{13}C$ showed values between -24.44 to -29.44‰. The relative abundance of odd long chain *n*-alkanes *vs*. total odd *n*-alkanes was higher than 50 % in most of the samples (on average 61.0 ± 9.3%). Similarly, long chain *n*-alcohols were largely predominant among total *n*-alcohols in all samples (on average 86.1 ± 5.0%) without any difference related to the treatment.

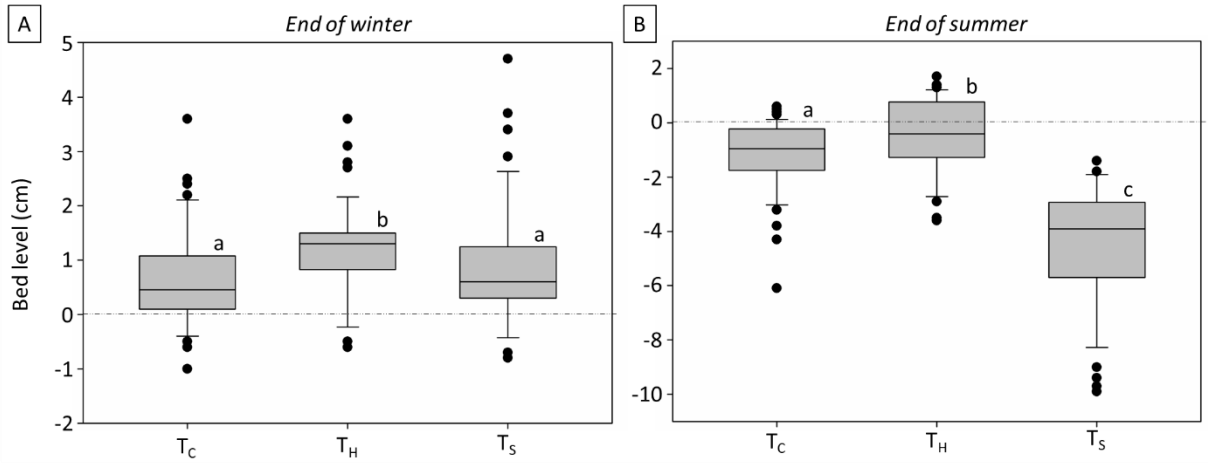

Figure 5. Bed level variation with averaged and quartile distribution by gathering all treatments (control: T_C, *H. diversicolor*: T_H, and *S. plana*: T_S) for the cold season (A) and at the end of the hot season (B). The lower-case letters on box plot correspond to the statistical groups, the groups being separated by a significant difference after a Tukey comparison tests.

Table 1. Significant differences observed between the values measured in the control treatment (T_C) and each of the others (T_N, T_H, and T_S) during the winter season. With average and standard deviation values as a function of *n* (given in the corresponding column). The stars given to values correspond to the significant difference with T_C (*p < 0.05*: *; *p < 0.01*: **; *p < 0.001*: ***) obtained using a Tukey comparison test or a non-parametric pairwise t-test.

Treatment	n	T_N	T_C	T_H	T_S
Bed level (cm)	48	n.d.	+ 0.66 ± 0.67	**+ 1.20 ± 0.58 *** **	+ 0.95 ± 0.83
Biological index (BIX)	3	**0.69 ± 0.00***	0.80 ± 0.00	0.72 ± 0.03	0.74 ± 0.02
Fluorescence index (FI)	3	**1.25 ± 0.01*****	1.43 ± 0.01	**1.24 ± 0.01*****	**1.26 ± 0.02*****
Nitrate reduction rates ($nmolNO_3^-$ cm^{-3} h^{-1})	15	32.4 ± 8.3	32.0 ± 8.7	**42.6 ± 3.7 ***	32.9 ± 7.4
Phaeopigments (%)	9	**54.7 ± 5.3***	45.1 ± 8.6	48.6 ± 8.5	47.7 ± 5.7
Colloidal carbohydrates EPS (µgEPS $gDSW^{-1}$)	9	14.6 ± 12.7	36.9 ± 10.5	18.8 ± 9.2	**13.9 ± 3.9****

3.2.2. Interstitial water parameters

In interstitial water samples, the DOC showed high values with on average 7.7 ± 1.9 mgC L^{-1} (supp. table 1). The DOM optical properties (illustrated from the fluorescence indices HIX, BIX and FI) highlighted a significant treatment effect for BIX and FI (table 1). The HIX index showed values lower than 5 for T_C while higher values were observed for T_N, T_H and T_S, reaching a maximum of about 8 for T_S (supp. table 1). The BIX values ranged between 0.69 and 0.80, with significant higher values for T_C (0.8) than other treatments (0.69 for T_N, 0.72 for T_H and 0.74 for T_S). The FI index showed similar trends as the BIX, with a significant difference between T_C (1.43) and the other treatments (around 1.25). In contrast, the different nutrient concentrations in pore water showed no significant differences between treatments (supp. table 1).

3.2.3. Biological related parameters

Overall, the microbial density in the sediment (bacteria and archaea) showed low values with no significant differences between treatment (on average $22.7 \times 10^4 \pm 9.7 \times 10^4$ microbial (*16S rRNA*) gene copy number per ng of extracted DNA; supp. table 1). Archaea made up 40.5 % of this total microbial community. Despite the differences observed in optical DOM properties, the microbial degradation activity illustrated through the CO_2 production rate showed no differences between treatments with on average 73.3 ± 10.8 nmol CO_2 $gDSW^{-1}$ h^{-1}. In contrast, the potential nitrate reduction rates showed significantly higher values in presence of *H. diversicolor* than in other treatments (on average 42.6 ± 3.7 nmol cm^{-3} h^{-1} for T_H *vs.* 32.1 ± 7.7 nmol NO_3^- cm^{-3} h^{-1} for the other ones; table 1). However, the density of denitrifiers in the sediment showed no significant differences with $4.1 \times 10^4 \pm 1.9 \times 10^4$ *nosZ* gene copy number per ng of extracted DNA. Despite the absence of significant differences, the treatment T_H showed the highest measured microbial activity and some of the highest values of microbial abundance (supp. table 1).

Regarding the parameters related to MPB, the chl *a* contents were low at this period with the highest values for T_N (3.5 ± 0.5 µg chl *a* gDW^{-1}) but without any significant differences with T_C, T_H and T_S which presented on average 2.7 ± 0.5 µg chl *a* gDW^{-1}. The colloidal carbohydrate EPS concentrations showed the highest values for T_C (36.9 ± 10.5 µgEPS $gDSW^{-1}$) and significant lower values for the macrofauna treatments with 13.9 ± 3.9 µg $gDSW^{-1}$ for T_S and 18.8 ± 9.2 µgEPS $gDSW^{-1}$ for T_H (table 1). The other EPS fractions showed no significant difference between treatments with on average a concentration of 45.6 ± 11.5 µg gDW^{-1} for bound carbohydrate EPS, and concentrations of 3.15 ± 0.6 and 7.12 ± 0.4 µg gDW^{-1} respectively for the colloidal and bound fractions of protein EPS. The percentage of phaeopigments relative to total photopigments showed a significant higher value in T_N (54.7 ± 5.3%) in comparison to T_C but no significant differences between control and macrofauna treatments was recorded with an average of 49.0 ± 7.7%. Photosynthetic parameters were constant between treatment with on average a F_V/F_M of 0.49 ± 0.07, an α of 0.37 ± 0.06 and a $rETR_{max}$ of 156 ± 49. The optimal irradiance (E_{opt}) was on average of 391 ± 239 µmol photons m^{-2} s^{-1} and the saturation coefficient of light (E_k) of 57 ± 17 µmol photons m^{-2} s^{-1}.

3.3. Late summer conditions

3.3.1. Sedimentary parameters

For each treatment (T_C, T_H, T_S), the bed level analysis revealed a global net erosion of the sediment (table 2; fig. 5-B). This erosion pattern was significantly stronger for T_S (-4.5 ± 1.8 cm) compared to other treatments

and significantly weaker for T_H (-0.5 ± 1.0 cm). In the presence of *S. plana*, the silt particles appeared in lower proportion than with other treatments (on average 22.9 ± 2.9% for T_S *vs.* in mean 30.4 ± 4.1% for T_H, T_C, and T_N). The other sedimentary parameters highlighted the same significant difference for T_S which showed a higher volumetric mass (1.95 ± 0.1 kg L^{-1}) and dry bulk density (1349.4 ± 30.3 kg m^{-3}), as well as a lower water content (36.4 ± 1.6%) than other treatments (table 2). The three other treatments showed on average a volumetric mass of 1.88 ± 0.1 kg L^{-1}, a dry bulk density of 1257.0 ± 43.8 kg m^{-3}, and a water content of 42.0 ± 2.8%.

Parameters related to the SedOM showed no significant differences between treatment with on average a TOC of 1.49 ± 0.43%, a TN of 0.18 ± 0.04%, and a $\delta^{13}C$ of -26.34‰. Sediment samples contained 63.6 ± 3.5% of odd long chain *n*-alkanes relative to total odd *n*-alkanes and 87.8 ± 2.3% of long chain *n*-alcohols among total *n*-alcohols (supp. table 2).

Table 2. Significant differences observed between the values measured in the control treatment (T_C) and each of the others (T_N, T_H, and T_S) during the late summer period. With average and standard deviation values as a function of *n* (given in the corresponding column). The stars given to values correspond to the significant difference with T_C (*p < 0.05*: *; *p < 0.01*: **; *p < 0.001*: ***) obtained using a Tukey comparison test or a non-parametric pairwise t-test.

Treatment	n	T_N	T_C	T_H	T_S
Bed level (cm)	48	n.d.	-1.18 ± 0.95	**-0.53 ± 1.05***	**- 4.49 ±1.78*****
Silt particles content (%)	9	30.7 ± 4.2	29.7 ± 4.5	30.7 ± 3.5	**22.9 ± 2.9***
Water content (%)	9	43.2 ± 2.5	41.42 ± 3.1	41.4 ± 2.6	**36.4 ± 1.6***
Dry bulk density (Csed: kg m^{-3})	9	1237.9 ± 39.0	1266.1 ± 49.0	1266.8 ± 42.8	**1349.4 ± 30.3***
Humification index (HIX)	3	7.30 ± 0.21	5.49 ± 0.16	6.97 ± 0.62	**7.76 ± 0.69***
Nitrate reduction rates ($nmolNO_3^-$ cm^{-3} h^{-1})	15	100.9 ± 13.0	95.4 ± 7.3	**77.2 ± 9.7***	**72.6 ± 8.7*****

3.3.2. Interstitial water parameters

In interstitial water samples, the DOC showed low values, with on average 4.2 ± 1.3 mgC L^{-1} without any differences between treatments (supp. table 2). The BIX and FI indices showed higher values for T_C (0.8 and 1.45, respectively) than for the other treatments (around 0.7 for BIX and 1.26 for FI). The HIX index showed a lower value, around 6, for T_C and values around 7 for T_H and above 7 for T_S and T_N. The different nutrient concentrations in pore water showed a high variability between replicates resulting in an absence of significance between treatments (supp. table 2).

3.3.3. Biological related parameters

The microbial density in the sediments (bacteria and archaea) showed lower *16S rRNA* gene copy numbers per ng of extracted DNA in T_S ($22.7 \times 10^4 \pm 1.2 \times 10^4$) compared to T_C, T_H, and T_N ($53.2 \times 10^4 \pm 26.2 \times 10^4$; supp. table 2). Archaea made up 49.8 % of the total microbial communities. This difference between treatment was also observed for the *nosZ* genes which showed a lower abundance in T_S ($6.0 \times 10^4 \pm 2.4 \times 10^4$) than in T_H and T_N ($8.3 \times 10^4 \pm 2.8 \times 10^4$). In terms of microbial activity, the potential nitrate reduction rates were significantly lower

in presence of macrofauna (T_S and T_H) than without (T_N and T_C) with respectively 74.9 ± 9.9 and 98.2 ± 10.8 nmol cm^{-3} h^{-1} (table 2). The CO_2 production rate showed no differences between treatments with on average 171.0 ± 24.2 nmol CO_2 gDW^{-1} h^{-1}.

Regarding the MPB related parameters, the chlorophyll *a* content showed a lower content for T_S with 4.2 ± 1.4 µg chl *a* $gDSW^{-1}$ while higher values were observed for T_C, T_H and T_N (in mean 6.4 ± 0.8 µg chl *a* $gDSW^{-1}$; supp. table 2). The same trend was observed when analysing chl *a* concentration in mg chla.m^{-2}. The colloidal carbohydrate EPS concentrations showed a significant difference between T_S (90.9 ± 6.6 µgEPS $gDSW^{-1}$) and T_H (77.5 ± 3.7 µgEPS $gDSW^{-1}$). The other EPS fractions showed no significant difference between treatments with on average a concentration of 171.4 ± 13.8 µg gDW^{-1} for bound carbohydrate EPS, and concentrations of 2.5 ± 0.8 and 3.2 ± 0.7 µg gDW^{-1} respectively for the colloidal and bound fractions of protein EPS. The percentage of phaeopigments relative to total photopigments also showed no significant differences with an average of 68.0 ± 4.7%. Regarding photosynthetic parameters, only the F_V/F_M showed significant lower values for T_S (0.42 ± 0.13) while the other treatments showed a mean value of 0.55 ± 0.07. The other photosynthetic parameters were similar between treatments with a mean value of 0.37 ± 0.11 and a mean $rETR_{max}$ of 97.1 ± 33.5. The optimal irradiance (E_{opt}) was on average of 530.6 ± 210 µmol photons m^{-2} s^{-1} and the saturation coefficient of light (E_k) of 305.4 ± 118.4 µmol photons m^{-2} s^{-1} (supp. table 2).

4. Discussion

The central hypothesis of this study posited that coexisting organisms, *Hediste diversicolor* and *Scrobicularia plana*, would exert antagonistic effects on sedimentary properties, biogeochemical processes, and microbial dynamics. Our results shed light on the more intricate dynamics governing intertidal mudflats. During winter conditions, the physical parameters, especially temperature and particles deposition, exert a more significant influence, overshadowing the role played by the presence of ecosystem engineers. No significant effects were observed with the presence of *Scrobicularia plana*. However, in an unexpected way, the presence of *Hediste diversicolor* slightly mitigated the impacts of the physical parameters. In late summer conditions, in line with our hypothesis, our results reveal that the presence of each bioturbator strongly exert a strong influence on both biotic and abiotic parameters, with opposite effects. The presence and activity of *S. plana* led to a complete disruption of the sediment matrix, resulting in negative impacts on associated biological and especially microbial processes. In contrast, the presence and activity of *H. diversicolor* contributed to maintaining the sediment matrix and enhanced the studied biogeochemical processes. Although more in-depth measurements of bioturbation processes and the use of more precise methods will be necessary to deepen the findings on specific processes, this interdisciplinary study confirms the significant influence of ecosystem engineers in mudflats and underscores the interconnected and cumulative nature of the consequences arising from their presence on all processes simultaneously.

4.1. Combined effects of temperature and presence of macrofauna in winter conditions.

In February, the sediment accretion in all treatments during the experiment revealed that deposition rates were stronger than erosion rates on the site. This is intricately linked to the dynamics of the estuary where currents induce erosion on the southern mudflats, and subsequently transport sediment particles towards the northern mudflats, leading predominantly to sediment accretion. This pattern being accentuated in winter by the higher

currents and the maximum turbidity zone located in the downstream estuary, reinforcing the amount of suspended particles (turbidity up to > 500 NTU; source: SYNAPSES network) that can settle on the upper mudflats of the estuary, especially during neap-tide periods (Le Hir et al. 2001). Thereby, it appears that the abiotic environment exerts a larger impact on the studied parameters variation than the macrofauna activities. This can be explain by the decrease of biological activities at low temperature (Georlette et al. 2004). The low temperatures that varied between -5.5 and 13.8 °C with frost events on the surface, are most likely responsible for the low measured microbial biomass, including bacteria, archaea, and MPB. For MPB, temperature is the most important factor explaining the seasonal variation of biomass and production rates (Blanchard et al. 1996). At low temperature, a decrease in the activity or deactivation of the enzymes involved in photosynthesis limits enzymatic activity by following the rules of the Arrhenius laws, consequently reducing MPB growth and primary production rates (Morgan-Kiss et al. 2006). For bacteria and archaea, frost and low temperatures on the sediment surface also play an important role in the biogeochemical process rates (Shen et al. 2020), the average microbial activity decreasing with the low temperatures, far from the optimum temperature of 15°C for production rates (Shen et al. 2015). The low temperatures also most likely resulted in a reduced activity for *S. plana* in T_S regarding motility, grazing, and respiration rates, which might explain the low influence of their presence. This ecosystem engineer is known to generate an intense sediment reworking (Wiesebron et al. 2021) that was not observed through the bed level variations under the low temperature of the present study. Moreover, no active siphons were visible on the site even in the bivalve-enriched units. This is supported by previous results showing that the fauna-mediation of the sediment matrix is regulated by temperature for bivalves with an optimal value between 24 and 30 °C for *S. plana* (Hughes 1969; Brey 2001; Cozzoli et al. 2018).

The observed significant differences between the treatment with the addition of *H. diversicolor* and the control, especially regarding bed accretion, suggest that the influence of this species on the surrounding environment was not inhibited by environmental factors. This resulted in cumulative effects of both winter conditions and bio-irrigation by this gallery-diffuser on the measured parameters. *H. diversicolor* can tolerate wide temperature fluctuations (Wolff 1973) with reduced food-searching activity only occurring below 8°C (Scaps 2002). Furthermore, its bioirrigation rates are not temperature-dependent (Sanz-Lázaro et al. 2011). This species inhabits burrows lined with mucus-filled galleries that extend over 10 cm into the sediment (Davey 1994). Temperature fluctuations at this depth tend to be more moderate, consistent with our observed temperature profiles, and explaining their tolerance to low environmental temperature. Therefore, it can be asserted that temperature during the winter manipulative experiment doesn't significantly decrease the activity of *H. diversicolor*, especially considering the insulating effect of their mucus secretions, known to confer resistance to cold conditions (Hawes et al. 2010). In addition to constructing mucus-lined galleries, *H. diversicolor* releases mucus during its feeding activities by using a mucous trapping-net even at a temperature of 5°C (Riisgård et al. 1992). This mucus secretion were shown to trap particles as much as during high tide where they behave as filter-feeders and at low tide where they switch to deposit-feeding (Esselink and Zwarts 1989; Esnault et al. 1990; Riisgard 1991a; Scaps 2002). These mucus secretions, functioning as sediment traps, most likely explain the significantly higher sediment accumulation observed in the T_H treatment. However, the mucus released by *H. diversicolor* at the sediment surface was not detected in our study, as no significant differences in EPS concentrations were observed between T_H and T_C (supp. table 1). Nonetheless, this multidisciplinary study revealed a notable impact of *H. diversicolor* on the microbial community. T_H treatments exhibited higher values for microbial-related parameters compared to

T_C and T_S (supp. table 1), indicating enhanced microbial growth and activity. The preference of microbes for EPS as a carbon source (Bouillon and Boschker 2006; Bellinger et al. 2009; Taylor et al. 2013; Morelle et al. 2022) likely led to rapid EPS consumption in the presence of *H. diversicolor*, resulting in non-detectable EPS levels. This assumption is further supported by the slightly higher average DOC values in T_H treatment compared to T_C (+7.7%) and T_S (+28.8%; supp. table 1), suggesting a higher degradation of labile OM (Perkins et al. 2022). Although not statistically significant, this aligns with slightly higher average NH_4^+ concentrations in pore water samples from T_H compared to T_C (+9%) and T_S (+5.6%; supp. table 1). Microbes involved in nitrate reduction appeared to benefit from the presence of *H. diversicolor*, as evidenced by the significantly higher nitrate reduction rates and, although not reaching statistical significance ($p = 0.13$), the slightly higher abundance of *nosZ* genes in T_H, respectively 48% and 42% higher than in T_S and T_C (supp. Table 1). This also aligns with the lower, though not statistically significant ($p = 0.7$), average in NO_3^- concentrations measured in the pore water samples from T_H with an average 15% lower than T_C (supp. table 1). This difference between T_H and the other treatments may be attributed to bioirrigation activities. As demonstrated in various sediment dwellers (e.g., bivalves, worms, crustaceans, echinids), bioturbation directly stimulates nutrient release at the sediment-water interface (Eriksson et al. 2017). Nematodes have also been shown to enhance bacterial activity and nutrient fluxes by frequently ventilating galleries across the sediment-water interface (D'Hondt et al. 2018). In our case, the bioirrigation performed by *H. diversicolor* (Kristensen and Hansen 1999) is known to enhance oxygen penetration, thereby promoting aerobic and anaerobic organic matter remineralization, which likely stimulated bacterial productivity and nutrient release (Richard et al. 2023). Even in winter conditions, when ventilation rates of *H. diversicolor* may decrease (Kristensen 1983; Riisgård et al. 1992; Vedel 1998), our results showed that their presence still exerts an influence on the surrounding environment.

Significantly higher values of EPS concentrations were observed in the control treatment (T_C) in concomitance with lower values of the humification index HIX and higher values of the fluorescence indices BIX and FI (table 1). The reworking, reshaping, and flattening of the sediments may have disturbed the sediment matrix and MPB biofilm. This hypothesis is confirmed by the significantly lower values of chl *a* measured in T_C, T_H, and T_S, in comparison to T_N (Table 1). In those conditions, MPB cells would have to build new pioneering biofilms by performing migration, this process occurring during a lag phase of several days (Yallop et al. 2000; Orvain et al. 2014). In T_C, the high values of carbohydrate EPS must have played a role in the migrating movement of epipelic benthic diatoms and contributed to the adhesion of microalgae at the sediment surfaces by forming biofilms. This was supported by the values of the fluorescence indices, suggesting the presence of a more freshly and microbially produced less aromatic DOM (McKnight et al. 2001) which could be attributed to a higher EPS production by MPB. This assumption was support by Li et al. (2023) showing that microbial EPS showed higher BIX and FI concomitant with lower HIX than more aromatic products with values in the range of our results. The absence of such trends in the treatments with macrofaunal addition (T_S and T_H) could be attributed to the feeding activity of the ecosystem engineers which, despite an apparent reduced activity for *S. plana*, must continue to feed on the OM pool.

4.2. Intense top-down impact of macrofauna in late summer conditions

In late summer, the addition of *S. plana* individuals led to a coarser sediment structure (table 2), suggesting that the reworking activity of the bivalves led to the bioresuspension of fine sediment particles. This is

confirmed by the temporal changes of the bed topography, which showed a significant loss by erosion in this treatment (fig. 5). In addition to particle size, the sediment reworking performed by *S. plana* also significantly affected most of the sedimentary parameters (volumetric mass, dry bulk density, and water content; table 2). These results highlight the considerable effects of the *S. plana* activities on the sedimentary matrix at this season. This is in line with the literature showing that the biological activity for bivalves and the related impacts on the sedimentary matrix are important and dependent on temperature (Brown et al. 2004; Cozzoli et al. 2020, 2021; Wiesebron et al. 2021). The modelled sediment loss resulting from *S. plana* activities was estimated at 50 cm $year^{-1}$ in the Marennes-Oléron Bay (Orvain et al. 2012). Considering the seasonal changes and the optima of this species for temperature, our results were in accordance with this estimation, showing an impact of *S. plana* on the sedimentary matrix corresponding to a sediment loss of 3 cm in 1 week. These effects were likely mainly due to the biological activities of *S. plana* related to burrowing and/or nutrition activities, which consist in siphoning the sediment surface that surrounds its semi-permanent burrow (Orvain 2005), continuously consuming the MPB during the low tide (Hughes 1969). The low chl *a* content measured in T_S could thereby most likely be due to an elevated foraging activity. However, in our study, the phaeopigment percentages, which represent the degraded compounds of chl *a*, were not different in T_S compared to other treatments (supp. table 2). Such a difference would have been expected as the result of a more intense predation pressure. The absence of effects on phaeopigments might be due to the rapid diffusion and/or resuspension of these pigments due to a high hydrodynamic stress as already suggested by Anand et al. (2014). This could also include resuspension of benthic diatoms, which in this case would apply to all treatments. In addition, the low chl *a* content could be an indirect effect of *S. plana* due to the strong disruption of the sediment matrix, which might limit the formation of structured MPB biofilms and in turn reduce photosynthesis and biomass production (Morelle et al. 2020). This assumption is supported by the lower values of the maximum effective quantum yield of the PSII (F_V/F_M) measured in T_S than in other treatments. Indeed, this result suggests that MPB was not in optimal conditions for photosynthesis since this rate depends on the physiological status of the biofilm (Serôdio et al. 2007). Such indirect negative impact of *S. plana* on the biological compartment was also observed in the microbial abundances and activity. Indeed, the T_S showed low microbial abundance both for bacteria and archaea (*16S rRNA* copy numbers) and the lowest activity in terms of nitrate reduction rates. This suggests that the presence of *S. plana* at such density (440 ind m^{-2}) in summer resulted in an intense sediment reworking almost completely inhibiting the biological components at the basis of the benthic trophic network of the intertidal mudflats. However, the present densities tested were the highest found for this species in the studied mudflat, and the activity of *S. plana* was somewhat slowed down by temperature (as seen in our winter results). Thereby, it's likely that this destructive impact is usually less pronounced compared to what we observed during our late-summer experiment. In addition, this effect must also be lower by the intense predation pressure that this bivalve receives from the upper compartment of the trophic network which can result in a strong reduction of siphon extension and feeding activity for bivalves (Maire et al. 2010).

In contrast, the treatment with *H. diversicolor* showed the lowest bed level erosion (fig. 5), thereby suggesting that the presence of polychaetes limit particle resuspension due to biostabilisation effects by mucus secretion which can result in a relative bed accretion (Riisgard 1991b; Passarelli et al. 2012). In this survey, since the sediment parameters were not significantly different compared to T_N and T_C, we suggest that the activity of *H. diversicolor* improved the stability of the sediments and, thus, attenuated the erosion, rather than promoting sediment accumulation. The fact that the presence of *H. diversicolor* reduced sediment erosion rates must also

have limited the MPB biofilm resuspension (Andersen et al. 2010; Donadi et al. 2013) and played a role in the high level of MPB biomass that was observed (table 2). Despite the predation pressure exerted by *H. diversicolor* (Scaps 2002), the chl *a* concentrations were similar to the natural and control treatments (T_N and T_C). This could be explained by a balance existing between the decrease in MPB biomass related to the feeding activity of *H. diversicolor* and the increase in the biomass related to their bioirrigation activities (Asmus and Bauerfeind 1994; Fernandes et al. 2006; Morelle et al. 2021; Richard et al. 2023). In the present case, enhancement of nutrients fluxes through bioirrigation of *H. diversicolor* (Kristensen and Hansen 1999) may have promoted bacterial productivity and MPB growth, which in turn may have decreased the vulnerability to erosion and promoted sediment accumulation through additional EPS production (Widdows et al. 2004; Andersen et al. 2010). Indeed, a higher abundance of both *16S rRNA* genes (bacteria, archaea) and *nosZ* genes (denitrifiers) was observed in the T_H treatments compared to T_C and T_N, suggesting a stimulation process of microbial growth by *H. diversicolor*. This might be due to a higher degradation rate of OM in the presence of *H. diversicolor* related to the higher oxygen penetration with bioirrigation activities (Pischedda et al. 2012). However, this potential increase in degradation activity was not observed in the microbial activity measured at the end of the experiment (CO_2 production and nitrate reduction rates) which showed higher values in T_C. Moreover, higher values of HIX as well as lower values of BIX and FI in T_H than in T_C suggest an increase in DOM aromaticity related to the presence of *H. diversicolor* and/or to the use, consumption, or transformation of components of lower aromaticity (Aller 1980; Zhang et al. 2022). Indeed, such an increase could be explained by the transfer of more degraded organic material from deeper sediment to the surface (also significant and pertinent for the T_S treatment). This is in line with the observations made by He et al. (2019), who showed that bioturbation activities accelerated the DOM release, mainly composed of aromatic/mature material (higher HIX), from sediment to overlying water with bioturbation. He et al. (2019) also reported changes in DOM composition over time, with an increase of microbially-produced DOM resulting from bacterial growth and propagation by bioturbation. In the present study, microbial production of DOM was not observed through the fluorescence indices, as the FI values corroborate a more terrestrial/mature character of DOM in the enriched treatments, in line with the HIX variations (table 2). Overall, the HIX and FI values were low and BIX values high, reflecting a mixture of organic material of low aromaticity and moderate to strong autochthonous sources with more mature and hydrophobic DOM components (Huguet et al. 2009). These results are consistent with those reported by Bowen et al. (2017) in the pore waters of California intertidal wetlands and by Burdige et al. (2004) in marine surface sediments, with autochthonous aquatic DOM predominant in surface waters and more terrestrial/refractory material in deeper pore waters. Nevertheless, the nature of sedimentary OM remains the same whatever the season and the treatment, with a strong terrestrial imprint. This is shown by both bulk and molecular analyses, with depleted $\delta^{13}C$ values of sedimentary OM and the predominance of long-chain *n*-alkanes and *n*-alcohols derived from terrestrial plants *vs.* short-chain homologues (Bianchi and Canuel 2011). Such results converge with the general view that terrestrial OM is refractory and well-preserved in sediments, in contrast with OM components produced *in situ*, considered as labile and less abundant in sediments (e.g., Burdige 2007). Nevertheless, the lower BIX values in T_H than in T_C suggested that the freshly produced DOM was used/consumed, degraded, or released in surficial water. Thereby, we assumed that, during the experiment, the presence of *H. diversicolor* stimulated the degradation of low aromatic compounds, as the latter are, by nature, more rapidly and easily degraded (Hansen et al. 2016). This is in line with the increase in microbial abundance and the decrease in DOM aromaticity (lower HIX) observed in T_H. The rapid depletion of easily degradable

compounds in pore waters, and the release of such compounds in surficial water favoured by bioirrigation of *H. diversicolor*, thus explain that the microbial production of DOM was not observed through the fluorescence analyses. Thereby, our results suggested that the activity of *H. diversicolor* had positive effects on both the sedimentary matrix and on microbial carbon fluxes, despite its high density and consequent predatory activity.

5. Conclusions

The influence of two intertidal bioturbators, *H. diversicolor* and *S. plana*, on the sedimentary, biogeochemical, and microbial dynamics was evaluated through field manipulative experiments during the two most contrasted seasons in a temperate estuarine mudflat. The present study confirmed the importance of temperature and water flow regimes both on macrofauna activity and microbial dynamics in intertidal mudflat. In the two different situations (either high sediment deposition and low temperature in winter, or high erosion and temperature under late summer conditions), the presence or absence of the bioturbators was shown to modify the sediment particle grain size composition and bed topography, with the erosion/accretion of the sediment partly related to the nutrition and burrowing activities of the species. The bioturbators were also observed to have a simultaneous influence on most of the studied parameters in the surficial sediment layer – with a direct or indirect impact on the pore water DOM quality, the growth, and activities of microorganisms (i.e., bacteria, archaea, and MPB). This study showed that some links between the different compartments are difficult to highlight without studying all components reinforcing the interest of conducting interdisciplinary studies to consider a maximum of biological and physicochemical variables to improve the understanding of ecosystem functioning. This study also highlights the importance of biological control of sedimentary systems on tidal flats, even in macrotidal estuaries. This is critical to improve management and conservation policies of estuarine ecosystems by better integrating the functional roles and bioturbation of dominating macrofauna, to restore the productivity of the intertidal zones, and to develop new models coupling biogeochemistry and benthic processes to sediment dynamics able to produce more realistic scenarios in the context of the global warming.

Acknowledgments:

This study was funded by the PHARESEE© project (Program GIP Seine-Aval 6) which aims to better understand, for modelling and restoration purposes, the links existing between hydrosedimentary, biogeochemical and microbial dynamics on mudflats ecosystems. The authors want to thank the GIP Seine-Aval agency, especially N. Bacq. Thank you to Jean Paul Lehodey (CREC) & Jean-Marc Paint (IUT Grand Ouest Normandie) for their help in the field systems conception and to the people who actively participated in sampling and/or analyses, especially Thomas Lecarpentier (Maison de l'Estuaire), Mathieu Chauveau, Guillaume Izabel, Guillaume Bouger, Amelie Gaigaerd, Cedric Fouillet, Véronique Vaury, Johanne Lebrun-Thauront, Kélina Judith, Jessica Maubert, Sarah Adeline, Théo Chiron, Camille Duchemin, Enora Logodin, Clémence Paucis, Amaury Tuon, Michel Simon and Romain Levaillant. We are also thankful to Virginie Daburon who performed genetic analyses of microbial DNA from sediment at the molecular ecology platform (UMR 6553 Ecobio, Rennes, CNRS/UR1), Marion Chorin for the nutrient analyses at the EcoChimie Platform (EcoChim) from UMS OSUR 3343, and David Moussa, chemical engineer at Rouen University (M2C-Rouen) for providing nutrients and TOC chemical analysis. Authors thank the support of CESAM (UIDP/50017/2020 + UIDB/50017/2020 + LA/P/0094/2020).

References

Admiraal, W., and H. Peletier. 1980. Influence of Seasonal Variations of Temperature and Light on the Growth Rate of Cultures and Natural Populations of Intertidal Diatoms *. **2**: 35–43.

Aller, R. C. 1980. Diagenetic Processes Near the Sediment-Water Interface of Long Island Sound. I.: Decomposition and Nutrient Element Geochemistry (S, N, P), p. 237–350. *In* B.B.T.-A. in G. Saltzman [ed.], Estuarine Physics and Chemistry: Studies in Long Island Sound. Elsevier.

Aller, R. C. 1988. Benthic fauna and biogeochemical processes in marine sediments: The role of burrow structures. Nitrogen Cycl. Coast. Mar. Environ. 301–341.

Aller, R. C., and J. K. Cochran. 2019. The critical role of bioturbation for particle dynamics, priming potential, and organic c remineralization in marine sediments: Local and basin scales. Front. Earth Sci. **7**: 1–14. doi:10.3389/feart.2019.00157

Anand, S. S., K. J. Anju, D. Mathew, and M. D. Kumar. 2014. Sub-hourly changes in biogeochemical properties in surface waters of Zuari estuary, Goa. Environ. Monit. Assess. **186**: 719–724. doi:10.1007/s10661-013-3410-1

Andersen, T. J., M. Lanuru, C. Van Bernem, M. Pejrup, and R. Riethmueller. 2010. Erodibility of a mixed mudflat dominated by microphytobenthos and Cerastoderma edule, East Frisian Wadden Sea, Germany. Estuar. Coast. Shelf Sci. **87**: 197–206. doi:10.1016/j.ecss.2009.10.014

Asmus, R. M., and E. Bauerfeind. 1994. The microphytobenthos of Königshafen - spatial and seasonal distribution on a sandy tidal flat. Helgolander Meeresuntersuchungen **48**: 257–276.

Behrenfeld, M. J., O. Prasil, M. Babin, and F. Bruyant. 2004. in Search of a Physiological Basis for Covariations in Light-Limited and Light-Saturated Photosynthesis1. J. Phycol. **40**: 4–25. doi:10.1046/j.1529-8817.2004.03083.x

Bellinger, B. J., G. J. C. Underwood, S. E. Ziegler, and M. R. Gretz. 2009. Significance of diatom-derived polymers in carbon flow dynamics within estuarine biofilms determined through isotopic enrichment. Aquat. Microb. Ecol. **55**: 169–187. doi:10.3354/ame01287

Bianchi, T. S., and E. A. Canuel. 2011. Chemical biomarkers in aquatic ecosystems, Princeton University Press.

Blanchard, G. F., J.-M. Guarini, P. Richard, P. Gros, and F. Mornet. 1996. Quantifying the short-term temperature effect on light-saturated photosynthesis of intertidal mircophytobenthos. Mar Ecol Prog Ser **134**: 309–313. doi:10.3354/meps134309

Boudreau, B. P., and B. B. Jorgensen. 2001. The benthic boundary layer: Transport processes and biogeochemistry, Oxford Uni. Oxford University Press.

Bouillon, S., and H. T. S. Boschker. 2006. Bacterial carbon sources in coastal sediments: a review based on stable isotope data of biomarkers. Biogeosciences **3**: 175–185. doi:10.5194/bgd-2-1617-2005

Bowen, J. C., C. D. Clark, J. K. Keller, and W. J. De Bruyn. 2017. Optical properties of chromophoric dissolved organic matter (CDOM) in surface and pore waters adjacent to an oil well in a southern California salt marsh. Mar. Pollut. Bull. **114**: 157–168. doi:10.1016/j.marpolbul.2016.08.071

Bradford, M. M. 1976. A rapid and sensitive method for the quantitation of microgram quantities of protein utilizing the principle of protein-dye binding. Anal. Biochem. **72**: 248–254.

Brey, T. 2001. Population dynamics in benthic invertebrates. A virtual handbook. http//www. awi-bremerhaven. de/Benthic/Ecosystem/FoodWeb/Handbook/main. html. Alfred Wegener Inst. Polar Mar. Res. Ger.

774 Brown, J. H., J. F. Gillooly, A. P. Allen, V. M. Savage, and G. B. West. 2004. Response to Forum Commentary
775 on " Toward a Metabolic Theory of Ecology ". Ecology **85**: 1818–1821.
776 Bruno, J. F., and M. Bertness. 2001. Habitat modification and facilitation in benthic marine communities. Mar.
777 community Ecol.
778 Burdige, D. J. 2007. Preservation of organic matter in marine sediments: Controls, mechanisms, and an imbalance
779 in sediment organic carbon budgets? Chem. Rev. **107**: 467–485. doi:10.1021/cr050347q
780 Burdige, D. J., S. W. Kline, and W. Chen. 2004. Fluorescent dissolved organic matter in marine sediment pore
781 waters. Mar. Chem. **89**: 289–311. doi:10.1016/j.marchem.2004.02.015
782 Burdige, D. J., and T. Komada. 2015. Sediment Pore Waters, p. 535–577. *In* D.A. Hansell and C.A. Carlson [eds.],
783 Biogeochemistry of marine dissolved organic matter. Burlington: Academic Press.
784 Cartaxana, P., M. Ruivo, C. Hubas, I. Davidson, J. Serôdio, and B. Jesus. 2011. Physiological versus behavioral
785 photoprotection in intertidal epipelic and epipsammic benthic diatom communities. J. Exp. Mar. Bio. Ecol.
786 **405**: 120–127. doi:10.1016/j.jembe.2011.05.027
787 Chennu, A., P. Färber, G. De'ath, D. De Beer, and K. E. Fabricius. 2017. A diver-operated hyperspectral imaging
788 and topographic surveying system for automated mapping of benthic habitats. Sci. Rep. **7**: 1–12.
789 doi:10.1038/s41598-017-07337-y
790 Chennu, A., N. Volkenborn, D. De Beer, D. S. Wethey, S. A. Woodin, and L. Polerecky. 2015. Effects of
791 bioadvection by Arenicola marina on microphytobenthos in permeable sediments. PLoS One **10**: 1–16.
792 doi:10.1371/journal.pone.0134236
793 Claquin, P., I. Probert, S. Lefebvre, and B. Veron. 2008. Effects of temperature on photosynthetic parameters and
794 TEP production in eight species of marine microalgae. Aquat. Microb. Ecol. **51**: 1–11.
795 doi:10.3354/ame01187
796 Coffinet, S., A. Huguet, C. Anquetil, and others. 2017. Evaluation of branched GDGTs and leaf wax n-alkane δ2H
797 as (paleo) environmental proxies in East Africa. Geochim. Cosmochim. Acta **198**: 182–193.
798 doi:10.1016/j.gca.2016.11.020
799 Van Colen, C., F. Montserrat, M. Vincx, P. M. J. Herman, T. Ysebaert, and S. Degraer. 2010. Macrobenthos
800 recruitment success in a tidal flat: Feeding trait dependent effects of disturbance history. J. Exp. Mar. Bio.
801 Ecol. **385**: 79–84. doi:10.1016/j.jembe.2010.01.009
802 Colijn, F., and K. S. Dijkema. 1981. Species Composition of Benthic Diatoms and Distribution of Chlorophyll a
803 on an Intertidal Flat in the Dutch Wadden Sea. Mar. Ecol. Prog. Ser. **4**: 9–21.
804 Cozzoli, F., T. J. Bouma, P. Ottolander, M. S. Lluch, T. Ysebaert, and P. M. J. Herman. 2018. The combined
805 influence of body size and density on cohesive sediment resuspension by bioturbators. Sci. Rep. **8**: 1–12.
806 doi:10.1038/s41598-018-22190-3
807 Cozzoli, F., T. Gomes da Conceição, J. Van Dalen, and others. 2020. Biological and physical drivers of bio-
808 mediated sediment resuspension: A flume study on Cerastoderma edule. Estuar. Coast. Shelf Sci. **241**.
809 doi:10.1016/j.ecss.2020.106824
810 Cozzoli, F., M. Shokri, T. Gomes da Conceição, and others. 2021. Modelling spatial and temporal patterns in
811 bioturbator effects on sediment resuspension: A biophysical metabolic approach. Sci. Total Environ. **792**:
812 148215. doi:10.1016/j.scitotenv.2021.148215
813 Crain, C. M., and M. D. Bertness. 2006. Ecosystem Engineering across Environmental Gradients : Implications

for Conservation and Management. Bioscience **56**: 211–218.

D'Hondt, A. S., W. Stock, L. Blommaert, T. Moens, and K. Sabbe. 2018. Nematodes stimulate biomass accumulation in a multispecies diatom biofilm. Mar. Environ. Res. **140**: 78–89. doi:10.1016/j.marenvres.2018.06.005

Dauwe, B., P. M. J. Herman, and C. H. R. Heip. 1998. Community structure and bioturbation potential of macrofauna at four North Sea stations with contrasting food supply. Mar. Ecol. Prog. Ser. **173**: 67–83. doi:10.3354/meps173067

Davey, J. T. 1994. The architecture of the burrow of Nereis diversicolor and its quantification in relation to sediment-water exchange. J. Exp. Mar. Bio. Ecol. **179**: 115–129. doi:10.1016/0022-0981(94)90020-5

Davison, I. R. 1991. Environmental Effects on Algal Photosynthesis: Temperature. J. Phycol. **27**: 2–8. doi:10.1111/1529-8817.ep10868724

Derrien, M., K. H. Shin, and J. Hur. 2019. Biodegradation-induced signatures in sediment pore water dissolved organic matter: Implications from artificial sediments composed of two contrasting sources. Sci. Total Environ. **694**: 133714. doi:10.1016/j.scitotenv.2019.133714

Donadi, S., J. Westra, E. J. Weerman, and others. 2013. Non-trophic Interactions Control Benthic Producers on Intertidal Flats. Ecosystems **16**: 1325–1335. doi:10.1007/s10021-013-9686-8

Dubois, M., K. A. Gilles, J. K. Hamilton, Pa. Rebers, and F. Smith. 1956. Colorimetric method for determination of sugars and related substances. Anal. Chem. **28**: 350–356.

Eglinton, G., and R. J. Hamilton. 1967. Leaf epicuticular waxes. Science (80-.). **156**: 1322–1335.

Einfeldt, A. L., J. R. Doucet, and J. A. Addison. 2014. Phylogeography and cryptic introduction of the ragworm Hediste diversicolor (Annelida, Nereididae) in the Northwest Atlantic. Invertebr. Biol. **133**: 232–241. doi:10.1111/ivb.12060

Eriksson, B. K., J. Westra, I. Van Gerwen, and others. 2017. Facilitation by ecosystem engineers enhances nutrient effects in an intertidal system. Ecosphere **8**. doi:10.1002/ecs2.2051

Esnault, G., C. Retiere, and R. Lambert. 1990. Food resource partitioning in a population of Nereis diversicolor (Annelida, Polychaeta) under experimental conditions. Trophic Relationships Mar. Environ. **453467**: 453–467.

Esselink, P., and L. Zwarts. 1989. Seasonal trend in burrow depth and tidal variation in feeding activity of Nereis diversicolor. Mar. Ecol. Prog. Ser. **56**: 243–254.

Fanjul, E., M. Escapa, D. Montemayor, M. Addino, M. F. Alvarez, M. A. Grela, and O. Iribarne. 2015. Effect of crab bioturbation on organic matter processing in South West Atlantic intertidal sediments. J. Sea Res. **95**: 206–216. doi:10.1016/j.seares.2014.05.005

Fernandes, S., P. Sobral, and M. H. Costa. 2006. Nereis diversicolor effect on the stability of cohesive intertidal sediments. Aquat. Ecol. **40**: 567–579. doi:10.1007/s10452-005-8000-z

François, F., M. Gerino, G. Stora, J. P. Durbec, and J. C. Poggiale. 2002. Functional approach to sediment reworking by gallery-forming macrobenthic organisms: Modeling and application with the polychaete Nereis diversicolor. Mar. Ecol. Prog. Ser. **229**: 127–136. doi:10.3354/meps229127

Georlette, D., V. Blaise, T. Collins, and others. 2004. Some like it cold: Biocatalysis at low temperatures. FEMS Microbiol. Rev. **28**: 25–42. doi:10.1016/j.femsre.2003.07.003

Hansen, A. M., T. E. C. Kraus, B. A. Pellerin, J. A. Fleck, B. D. Downing, and B. A. Bergamaschi. 2016. Optical

properties of dissolved organic matter (DOM): Effects of biological and photolytic degradation. Limnol. Oceanogr. **61**: 1015–1032. doi:10.1002/lno.10270

Hawes, T. C., M. R. Worland, and J. S. Bale. 2010. Freezing in the Antarctic limpet, Nacella concinna. Cryobiology **61**: 128–132. doi:10.1016/j.cryobiol.2010.06.006

He, Y., B. Men, X. Yang, Y. Li, H. Xu, and D. Wang. 2019. Relationship between heavy metals and dissolved organic matter released from sediment by bioturbation/bioirrigation. J. Environ. Sci. (China) **75**: 216–223. doi:10.1016/j.jes.2018.03.031

Hellequin, E., C. Monard, A. Quaiser, M. Henriot, O. Klarzynski, and F. Binet. 2018. Specific recruitment of soil bacteria and fungi decomposers following a biostimulant application increased crop residues mineralization. PLoS One **13**: 1–19. doi:10.1371/journal.pone.0209089

Le Hir, P., A. Ficht, R. S. Jacinto, and others. 2001. Fine Sediment Transport and Accumulations at the Mouth of the Seine Estuary (France). Estuaries **24**: 950. doi:10.2307/1353009

Hope, J. A., D. M. Paterson, and S. F. Thrush. 2020. The role of microphytobenthos in soft-sediment ecological networks and their contribution to the delivery of multiple ecosystem services. J. Ecol. **108**: 815–830. doi:10.1111/1365-2745.13322

Hughes, R. N. 1969. A study of feeding in Scrobicularia plana. J. Mar. Biol. Assoc. United Kingdom **49**: 805–823.

Huguet, A., L. Vacher, S. Relexans, S. Saubusse, J. M. Froidefond, and E. Parlanti. 2009. Properties of fluorescent dissolved organic matter in the Gironde Estuary. Org. Geochem. **40**: 706–719. doi:10.1016/j.orggeochem.2009.03.002

Jones, C. G., J. H. Lawton, and M. Shachak. 1994. Organisms as ecosystem engineers. OIKOS **69**: 373–386.

Jones, C. M., D. R. H. Graf, D. Bru, L. Philippot, and S. Hallin. 2013. The unaccounted yet abundant nitrous oxide-reducing microbial community: A potential nitrous oxide sink. ISME J. **7**: 417–426. doi:10.1038/ismej.2012.125

Juneau, P., A. Barnett, V. Méléder, C. Dupuy, and J. Lavaud. 2015. Combined effect of high light and high salinity on the regulation of photosynthesis in three diatom species belonging to the main growth forms of intertidal flat inhabiting microphytobenthos. J. Exp. Mar. Bio. Ecol. **463**: 95–104. doi:10.1016/j.jembe.2014.11.003

Van De Koppel, J., T. Van Der Heide, A. H. Altieri, B. K. Eriksson, T. J. Bouma, H. Olff, and B. R. Silliman. 2015. Long-Distance Interactions Regulate the Structure and Resilience of Coastal Ecosystems. Ann. Rev. Mar. Sci. **7**: 139–158. doi:10.1146/annurev-marine-010814-015805

Kristensen, E. 1983. Ventilation and oxygen uptake by three species of. Mar. Ecol. Prog. Ser. **12**: 299–305.

Kristensen, E., G. Penha-lopes, M. Delefosse, T. Valdemarsen, C. O. Quintana, and G. T. Banta. 2012. What is bioturbation ? The need for a precise definition for fauna in aquatic sciences. **446**: 285–302. doi:10.3354/meps09506

Kristensen, K., and K. Hansen. 1999. Transport of carbon dioxide and ammonium in bioturbated (Nereis diversicolor) coastal, marine sediments. Biogeochemistry **45**: 147–168.

Laverman, A. M., P. Van Cappellen, D. Van Rotterdam-Los, C. Pallud, and J. Abell. 2006. Potential rates and pathways of microbial nitrate reduction in coastal sediments. FEMS Microbiol. Ecol. **58**: 179–192. doi:10.1111/j.1574-6941.2006.00155.x

Laverman, A. M., C. Pallud, J. Abell, and P. Van Cappellen. 2012. Comparative survey of potential nitrate and sulfate reduction rates in aquatic sediments. Geochim. Cosmochim. Acta **77**: 474–488.

doi:10.1016/j.gca.2011.10.033

Li, W., X. Li, C. Han, L. Gao, H. Wu, and M. Li. 2023. A new view into three-dimensional excitation-emission matrix fluorescence spectroscopy for dissolved organic matter. Sci. Total Environ. **855**: 158963. doi:10.1016/j.scitotenv.2022.158963

Lorenzen, C. J. 1967. Determination of Chlorophyll and Pheo-Pigments : Spectrophotometric Equations. Limnol. Oceanogr. **12**: 343–346. doi:10.4319/lo.1967.12.2.0343

Maire, O., J. N. Merchant, M. Bulling, L. R. Teal, A. Grémare, J. C. Duchêne, and M. Solan. 2010. Indirect effects of non-lethal predation on bivalve activity and sediment reworking. J. Exp. Mar. Bio. Ecol. **395**: 30–36. doi:10.1016/j.jembe.2010.08.004

Marchesi, J. R., T. Sato, A. J. Weightman, T. A. Martin, J. C. Fry, S. J. Hiom, and W. G. Wade. 1998. Design and evaluation of useful bacterium-specific PCR primers that amplify genes coding for bacterial 16S rRNA. Appl. Environ. Microbiol. **64**: 795–799. doi:10.1128/aem.64.2.795-799.1998

McKnight, D. M., E. W. Boyer, P. K. Westerhoff, P. T. Doran, T. Kulbe, and D. T. Andersen. 2001. Spectrofluorometric characterization of dissolved organic matter for indication of precursor organic material and aromaticity. Limnol. Oceanogr. **46**: 38–48. doi:10.4319/lo.2001.46.1.0038

Montserrat, F., C. Van Colen, P. Provoost, M. Milla, M. Ponti, K. Van den Meersche, T. Ysebaert, and P. M. J. Herman. 2009. Sediment segregation by biodiffusing bivalves. Estuar. Coast. Shelf Sci. **83**: 379–391. doi:10.1016/j.ecss.2009.04.010

Morelle, J., P. Claquin, and F. Orvain. 2020. Evidence for better microphytobenthos dynamics in mixed sand/mud zones than in pure sand or mud intertidal flats (Seine estuary, Normandy, France). PLoS One **15**: e0237211. doi:10.1371/journal.pone.0237211

Morelle, J., O. Maire, A. Richard, A. Slimani, and F. Orvain. 2021. Contrasted impact of two macrofaunal species (Hediste diversicolor and Scrobicularia plana) on microphytobenthos spatial distribution and photosynthetic activity at microscale. Mar. Environ. Res. **163**. doi:10.1016/j.marenvres.2020.105228

Morelle, J., C. Roose-Amsaleg, and A. M. Laverman. 2022. Microphytobenthos as a source of labile organic matter for denitrifying microbes. Estuar. Coast. Shelf Sci. **275**. doi:10.1016/j.ecss.2022.108006

Morelle, J., M. Schapira, F. Orvain, and others. 2018. Annual Phytoplankton Primary Production Estimation in a Temperate Estuary by Coupling PAM and Carbon Incorporation Methods. Estuaries and Coasts 1–19. doi:10.1007/s12237-018-0369-8

Morgan-Kiss, R. M., J. C. Priscu, T. Pocock, L. Gudynaite-Savitch, and N. P. A. Huner. 2006. Adaptation and Acclimation of Photosynthetic Microorganisms to Permanently Cold Environments. Microbiol. Mol. Biol. Rev. **70**: 222–252. doi:10.1128/MMBR.70.1.222-252.2006

Muyzer, G., E. C. De Waal, and A. G. Uitterlinden. 1993. Profiling of complex microbial populations by denaturing gradient gel electrophoresis analysis of polymerase chain reaction-amplified genes coding for 16S rRNA. Appl. Environ. Microbiol. **59**: 695–700. doi:10.1128/aem.59.3.695-700.1993

Oleszczuk, B., E. Michaud, N. Morata, P. E. Renaud, and M. Kędra. 2019. Benthic macrofaunal bioturbation activities from shelf to deep basin in spring to summer transition in the Arctic Ocean. Mar. Environ. Res. **150**: 104746. doi:10.1016/j.marenvres.2019.06.008

Orvain, F. 2005. A model of sediment transport under the influence of surface bioturbation: Generalisation to the facultative suspension-feeder Scrobicularia plana. Mar. Ecol. Prog. Ser. **286**: 43–56.

934 doi:10.3354/meps286043
935 Orvain, F., M. De Crignis, K. Guizien, S. Lefebvre, C. Mallet, E. Takahashi, and C. Dupuy. 2014. Tidal and
936 seasonal effects on the short-term temporal patterns of bacteria, microphytobenthos and exopolymers in
937 natural intertidal biofilms (Brouage, France). J. Sea Res.
938 Orvain, F., S. Lefebvre, J. Montepini, M. Sébire, A. Gangnery, and B. Sylvand. 2012. Spatial and temporal
939 interaction between sediment and microphytobenthos in a temperate estuarine macro-intertidal bay. Mar.
940 Ecol. Prog. Ser. **458**: 53–68.
941 Orvain, F., P. G. Sauriau, A. Sygut, L. Joassard, and P. Le Hir. 2004. Interacting effects of Hydrobia ulvae
942 bioturbation and microphytobenthos on the erodibility of mudflat sediments. Mar. Ecol. Prog. Ser. **278**: 205–
943 223. doi:10.3354/meps278205
944 Parlanti, E., K. Wörz, L. Geoffroy, and M. Lamotte. 2000. Dissolved organic matter fluorescence spectroscopy as
945 a tool to estimate biological activity in a coastal zone submitted to anthropogenic inputs. Org. Geochem. **31**:
946 1765–1781. doi:10.1016/S0146-6380(00)00124-8
947 Passarelli, C., C. Hubas, A. N. Segui, J. Grange, and T. Meziane. 2012. Surface adhesion of microphytobenthic
948 biofilms is enhanced under Hediste diversicolor (O.F. Müller) trophic pressure. J. Exp. Mar. Bio. Ecol. **438**:
949 52–60. doi:10.1016/j.jembe.2012.10.005
950 Paterson, D. M., I. Fortune, R. J. Aspden, and K. S. Black. 2019. Intertidal Flats: Form and Function, p. 383–406.
951 *In* Coastal Wetlands. Elsevier.
952 Perkins, A. K., I. R. Santos, A. L. Rose, K. G. Schulz, H. P. Grossart, B. D. Eyre, B. P. Kelaher, and J. M. Oakes.
953 2022. Production of dissolved carbon and alkalinity during macroalgal wrack degradation on beaches: a
954 mesocosm experiment with implications for blue carbon. Biogeochemistry **160**: 159–175.
955 doi:10.1007/s10533-022-00946-4
956 Pischedda, L., P. Cuny, J. L. Esteves, J. C. Poggiale, and F. Gilbert. 2012. Spatial oxygen heterogeneity in a
957 Hediste diversicolor irrigated burrow. Hydrobiologia **680**: 109–124. doi:10.1007/s10750-011-0907-x
958 Quaiser, A., X. Bodi, A. Dufresne, and others. 2014. Unraveling the stratification of an iron-oxidizing microbial
959 mat by metatranscriptomics. PLoS One **9**: 1–9. doi:10.1371/journal.pone.0102561
960 Raven, J., and R. J. Geider. 1988. Temperature and algal growth. New Phytol. **110**: 441–461. doi:10.1111/j.1469-
961 8137.1988.tb00282.x
962 Redzuan, N. S., and G. J. C. Underwood. 2021. The importance of weather and tides on the resuspension and
963 deposition of microphytobenthos (MPB) on intertidal mudflats. Estuar. Coast. Shelf Sci. **251**.
964 doi:10.1016/j.ecss.2021.107190
965 Richard, A., F. Orvain, J. Morelle, and others. 2023. Impact of Sediment Bioturbation on Microphytobenthic
966 Primary Producers: Importance of Macrobenthic Functional Traits. Ecosystems **26**: 1077–1094.
967 doi:10.1007/s10021-022-00817-x
968 Riisgard, H. U. 1991a. Suspension feeding in the polychaete Nereis diversicolor. Mar. Ecol. Prog. Ser. **70**: 29–37.
969 doi:10.3354/meps070029
970 Riisgard, H. U. 1991b. Suspension feeding in the polychaete Nereis diversicolor. Mar. Ecol. Prog. Ser. **70**: 29–37.
971 doi:10.3354/meps070029
972 Riisgård, H., A. Vedel, H. Boye, and P. Larsen. 1992. Filter-net structure and pumping activity in the polychaete
973 Nereis diversicolor: effects of temperature and pump-modelling. Mar. Ecol. Prog. Ser. **83**: 79–89.

974 doi:10.3354/meps083079
975 Santos, S., P. C. Luttikhuizen, J. Campos, C. H. R. Heip, and H. W. van der Veer. 2011. Spatial distribution
976 patterns of the peppery furrow shell Scrobicularia plana (da Costa, 1778) along the European coast: A
977 review. J. Sea Res. **66**: 238–247. doi:10.1016/j.seares.2011.07.001
978 Sanz-Lázaro, C., T. Valdemarsen, A. Marín, and M. Holmer. 2011. Effect of temperature on biogeochemistry of
979 marine organic-enriched systems: Implications in a global warming scenario. Ecol. Appl. **21**: 2664–2677.
980 doi:10.1890/10-2219.1
981 Scaps, P. 2002. A review of the biology, ecology and potential use of the common ragworm Hediste diversicolor
982 (O.F. Müller) (Annelida: Polychaeta). Hydrobiologia **470**: 203–218.
983 Seeberg-Elverfeldt, J., M. Schlüter, T. Feseker, and M. Kölling. 2005. Rhizon sampling of porewaters near the
984 sediment-water interface of aquatic systems. Limnol. Oceanogr. Methods **3**: 361–371.
985 doi:10.4319/lom.2005.3.361
986 Serôdio, J., S. Vieira, and F. Barroso. 2007. Relationship of variable chlorophyll fluorescence indices to
987 photosynthetic rates in microphytobenthos. Aquat. Microb. Ecol. **49**: 71–85. doi:10.3354/ame01129
988 Shen, Q., F. Ji, J. Wei, D. Fang, Q. Zhang, L. Jiang, A. Cai, and L. Kuang. 2020. The influence mechanism of
989 temperature on solid phase denitrification based on denitrification performance, carbon balance, and
990 microbial analysis. Sci. Total Environ. **732**. doi:10.1016/j.scitotenv.2020.139333
991 Shen, Z., J. Hu, J. Wang, and Y. Zhou. 2015. Biological denitrification using starch/polycaprolactone blends as
992 carbon source and biofilm support. Desalin. Water Treat. **54**: 609–615. doi:10.1080/19443994.2014.885395
993 Stal, L. J. 2010. Microphytobenthos as a biogeomorphological force in intertidal sediment stabilization. Ecol. Eng.
994 **36**: 236–245. doi:10.1016/j.ecoleng.2008.12.032
995 Stal, L. J., and J. F. C. de Brouwer. 2003. Biofilm formation by benthic diatoms and their influence on the
996 stabilization of intertidal mudflats. Berichte – Forschungszentrum Terramare **12**: 109–111.
997 Swanberg, I. L. 1991. The influence of the filter-feeding bivalve Cerastoderma edule L . on microphytobenthos :
998 a laboratory study. J. Exp. Mar. Bio. Ecol. **151**: 93–111.
999 Takai, K., and K. Horikoshi. 2000. Rapid detection and quantification of members of the archaeal community by
1000 quantitative PCR using fluorogenic probes. Appl. Environ. Microbiol. **66**: 5066–5072.
1001 doi:10.1128/AEM.66.11.5066-5072.2000
1002 Taylor, J. D., B. A. McKew, A. Kuhl, T. J. McGenity, and G. J. C. Underwood. 2013. Microphytobenthic
1003 extracellular polymeric substances (EPS) in intertidal sediments fuel both generalist specialist EPS-
1004 degrading bacteria. Limnol. Oceanogr. **58**: 1463–1480. doi:10.4319/lo.2013.58.4.1463
1005 Thibault, A., S. Derenne, E. Parlanti, and others. 2019. Dynamics of organic matter in the Seine Estuary (France):
1006 Bulk and structural approaches. Mar. Chem. **212**: 108–119. doi:10.1016/j.marchem.2019.04.007
1007 Ubertini, M., S. Lefebvre, A. Gangnery, K. Grangeré, R. Le Gendre, and F. Orvain. 2012. Spatial variability of
1008 benthic-pelagic coupling in an estuary ecosystem: consequences for microphytobenthos resuspension
1009 phenomenon. PLoS One **7**: e44155. doi:10.1371/journal.pone.0044155
1010 Underwood, G. J. C. 1994. Seasonal and spatial variation in epipelic diatom assemblages in the severn estuary.
1011 Diatom Res. **9**: 451–472. doi:10.1080/0269249X.1994.9705319
1012 Underwood, G. J. C., and J. C. Kromkamp. 1999. Primary Production by Phytoplankton and Microphytobenthos
1013 in Estuaries. Adv. Ecol. Res. **29**: 93–153. doi:10.1016/S0065-2504(08)60192-0

Vedel, A. 1998. Phytoplankton depletion in the benthic boundary layer caused by suspension-feeding Nereis diversicolor (Polychaeta):grazing impact and effect of temperature. Mar. Ecol. Prog. Ser. **171**: 125–132. doi:10.3354/meps171125

Vonk, J. E., B. E. van Dongen, and Ö. Gustafsson. 2008. Lipid biomarker investigation of the origin and diagenetic state of sub-arctic terrestrial organic matter presently exported into the northern Bothnian Bay. Mar. Chem. **112**: 1–10. doi:10.1016/j.marchem.2008.07.001

Weerman, E. J., P. M. J. Herman, and J. Van De Koppel. 2011. Macrobenthos abundance and distribution on a spatially patterned intertidal flat. Mar. Ecol. Prog. Ser. **440**: 95–103. doi:10.3354/meps09332

Widdows, J., A. Blauw, C. H. R. Heip, and others. 2004. Role of physical and biological processes in sediment dynamics of a tidal flat in Westerschelde Estuary, SW Netherlands. Mar. Ecol. Prog. Ser. **274**: 41–56.

Wiesebron, L. E., N. Steiner, C. Morys, T. Ysebaert, and T. J. Bouma. 2021. Sediment Bulk Density Effects on Benthic Macrofauna Burrowing and Bioturbation Behavior. Front. Mar. Sci. **8**: 1–16. doi:10.3389/fmars.2021.707785

Wolff, W. J. 1973. The estuary as a habitat: an analysis of data on the soft-bottom macrofauna of the estuarine area of the rivers Rhine, Meuse and Scheldt. Zool. Verkan. **126**: 1–242.

Yallop, M. L., D. M. Paterson, and P. Wellsbury. 2000. Interrelationships between rates of microbial production, exopolymer production, microbial biomass, and sediment stability in biofilms of intertidal sediments. Microb. Ecol. **39**: 116–127. doi:10.1007/s002489900186

Zhang, Y., J. Wang, J. Tao, and others. 2022. Concentrations of dissolved organic matter and methane in lakes in Southwest China: Different roles of external factors and in-lake biota. Water Res. **225**: 119190. doi:10.1016/j.watres.2022.119190

Zsolnay, A., E. Baigar, M. Jimenez, B. Steinweg, and F. Saccomandi. 1999. Differentiating with fluorescence spectroscopy the sources of dissolved organic matter in soils subjected to drying. Chemosphere **38**: 45–50. doi:10.1016/S0045-6535(98)00166-0

Zwarts, L., A.-M. Blomert, P. Spaak, and B. De Vriers. 1994. Feeding radius, burying depth and siphon size of Macoma balthica and Scrobicularia plana. J. Exp. Bot. **183**: 193–212.